



September 2019

Report No. 19-007

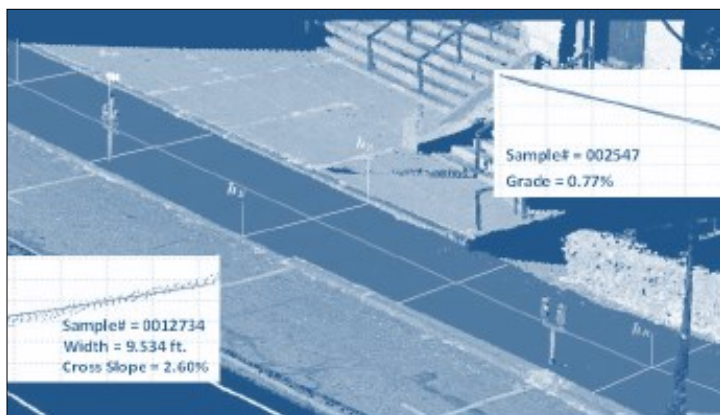
Charles D. Baker
Governor

Karyn E. Polito
Lieutenant Governor

Stephanie Pollack
MassDOT Secretary & CEO

Improving Pedestrian Infrastructure Inventory in Massachusetts Using Mobile LiDAR

Principal Investigator
Dr. Chengbo Ai
University of Massachusetts Amherst



Research and Technology Transfer Section
MassDOT Office of Transportation Planning



U.S. Department of Transportation
Federal Highway Administration

Technical Report Document Page

1. Report No. 19-007	2. Government Accession No.	3. Recipient's Catalog No.	
4. Title and Subtitle Improving Pedestrian Infrastructure Inventory in Massachusetts Using Mobile LiDAR		5. Report Date September 2019	
		6. Performing Organization Code	
7. Author(s) Chengbo Ai and Qing Hou		8. Performing Organization Report No. 19-007	
9. Performing Organization Name and Address University of Massachusetts Amherst 130 Natural Resources Way, Amherst, MA 01003		10. Work Unit No. (TRAIS)	
		11. Contract or Grant No.	
12. Sponsoring Agency Name and Address Massachusetts Department of Transportation Office of Transportation Planning Ten Park Plaza, Suite 4150, Boston, MA 02116		13. Type of Report and Period Covered Final Report - September 2019 [Nov. 2019 – Sept. 2019]	
		14. Sponsoring Agency Code n/a	
15. Supplementary Notes			
16. Abstract Pedestrian infrastructure is one of the most vital transportation infrastructures for pedestrians and wheelchair users who rely on quality sidewalks to facilitate safe and uninterrupted trips in their everyday lives. To meet the obligations of the Americans with Disabilities Act (ADA) Transition Plan and to make informed investment decisions in transportation asset management, MassDOT is actively seeking to improve data on existing pedestrian infrastructure to better understand the needs for maintenance and construction of pedestrian facilities. This study develops a new pedestrian infrastructure inventory and geometry measurement method by leveraging emerging mobile light detection and ranging (LiDAR), deep learning, and computer vision technologies, consisting of two computer-aided algorithms with measurements for sidewalk inventory and curb ramp inventory. The experimental tests conducted on the complete State Route 9 show that mobile LiDAR is an effective and efficient technology for network-level pedestrian infrastructure inventory. More than 85 miles of sidewalk and a total 1,297 curb ramps along State Route 9 were inventoried at the rates of 7.0 min/mile and 2.2 min/mile, respectively. This study also establishes a complete LiDAR point cloud processing pipeline (including algorithms, tools, and procedures) for many other critical transportation assets.			
17. Key Word Sidewalk, LiDAR, Pedestrian Infrastructure, Automation, Asset Management		18. Distribution Statement	
19. Security Classif. (of this report) unclassified	20. Security Classif. (of this page) unclassified	21. No. of Pages 53	22. Price n/a

Form DOT F 1700.7 (8-72)

Reproduction of completed page authorized

This page left blank intentionally.

**Massachusetts Department of Transportation (MassDOT)
and
University of Massachusetts Amherst**

**Improving Pedestrian Infrastructure Inventory in Massachusetts
Using Mobile LiDAR**

Final Report

Prepared By:

Dr. Chengbo Ai
Principal Investigator
chengbo.ai@umass.edu

Qing Hou
Research Assistant
qhou@umass.edu

Civil and Environmental Engineering
University of Massachusetts Amherst
130 Natural Resources Rd., Amherst, MA 01003

Prepared For:

Massachusetts Department of Transportation
Office of Transportation Planning
Ten Park Plaza, Suite 4150
Boston, MA 02116

September 2019

This page left blank intentionally.

Acknowledgments

Prepared in cooperation with the Massachusetts Department of Transportation, Office of Transportation Planning, and the United States Department of Transportation, Federal Highway Administration.

The Project Team would like to acknowledge the efforts of Jack Moran and his team from the Highway Division at MassDOT for providing technical support and oversight for this project, and Lily Oliver, Nicholas Zavolas, Quinn Molloy and Jose Simo from the Office of Transportation Planning at MassDOT, for providing necessary data and constructive suggestions for this project.

The Project Team would also like to acknowledge the effort of Matt Mann and Kimberley Foster from the University of Massachusetts Transportation Center for their administrative supports.

Disclaimer

The contents of this report reflect the views of the author(s), who are responsible for the facts and the accuracy of the data presented herein. The contents do not necessarily reflect the official view or policies of the Massachusetts Department of Transportation or the Federal Highway Administration. This report does not constitute a standard, specification, or regulation.

This page left blank intentionally.

Table of Contents

Technical Report Document Page	i
Acknowledgments	v
Disclaimer	v
Table of Contents	vii
List of Tables	ix
List of Figures	ix
1 Introduction	1
1.1 Background	1
1.2 Objectives and Detailed Work Tasks	2
1.3 Organization of this Report	3
2 Research Methodology	5
2.1 Literature Review	5
2.1.1 Existing Efforts of Sidewalk Inventory	5
2.1.2 Technologies and Methods for Sidewalk Inventory	7
2.1.3 Current Efforts of Sidewalk Inventory in MassDOT	13
2.2 Methodology Overview	15
2.3 Data Acquisition	16
2.4 Point Cloud Segmentation	17
2.4.1 PointNet	18
2.4.2 PointNet++	19
2.4.3 PointNet++ Model Training	21
2.4 Sidewalk Extraction	24
2.5 Curb Ramp Extraction	26
2.5.1 Automated Curb Ramp Extraction	26
2.5.2 Manual Curb Ramp Extraction	27
2.6 Key Feature Measurement	28
2.6.1 Sidewalk Features	28
2.6.2 Curb Ramp Feature	29
3 Results	30
3.1 Results of Acquired Data	30
3.2 Results for Sidewalk Inventory	30
3.2.1 Updated Sidewalk Locations	31
3.2.2 Updated Sidewalk Measures	32
3.2.3 Feasibility and Productivity	33
3.3 Results for Curb Ramp Inventory	34
3.3.1 Updated Curb Ramp Locations	34
3.3.2 Feasibility and Productivity	35
4 Conclusion	38
5 References	40

This page left blank intentionally.

List of Tables

Table 1 Basic environment of the road scene segmentation based on PointNet++	22
--	----

List of Figures

Figure 1 Flowcharts for Steps 1 and 2 of the sidewalk extraction algorithm (Balado et al., 2018)	9
Figure 2 Flowchart of the proposed road feature extraction algorithm (Soilán et al., 2018)	10
Figure 3 Illustration of the 2-D LiDAR scan-based segmentation algorithm (Ai and Tsai, 2016b)	11
Figure 4 The process of the cross-section segmentation connection method (Ai and Tsai, 2016b).....	12
Figure 5 A screenshot of the RIF data field (in brown) and the Curb Ramp data fields (in blue)	14
Figure 6 Illustration of the SR9 corridor of interest for this research project	15
Figure 7 Overview of the research methodology	16
Figure 8 Mobile LiDAR installations for both vertical and horizontal configuration.....	17
Figure 9 PointNet Architecture	18
Figure 10 PointNet++ Architecture (Qi et al., 2017).....	20
Figure 11 Illustrations of MSG and MRG2 (Qi et al., 2017)	21
Figure 12 Examples of the six classification classes	22
Figure 13 Accuracy, IoU, and IoU of each class per epoch	23
Figure 14 Illustrations for the splitting and merging algorithm	25
Figure 15 An example of the strip-based sidewalk extraction results	26
Figure 16 Illustrations of the results from the root filter (blue) and parts filter (orange).....	27
Figure 17 The interface of the manual curb ramp extraction tool	27
Figure 18 Illustrations of the sidewalk measurements for width, cross slope, and grade	28
Figure 19 Examples for various running slopes of curb ramps	29
Figure 20 An example of the collected mobile LiDAR point cloud.....	30
Figure 21 Example of the detected sidewalks in the urban, suburban and rural regions.....	32
Figure 22 An example of the measurements along a 1000-ft. section.....	33
Figure 23 An example of the updated curb ramp locations.....	35

This page left blank intentionally.

1 Introduction

This study of “Improving Pedestrian Infrastructure Inventory in Massachusetts Using Mobile LiDAR” was undertaken as part of the Massachusetts Department of Transportation (MassDOT) Research Program. This program is funded with Federal Highway Administration (FHWA) State Planning and Research (SPR) funds. Through this program, applied research is conducted on topics of importance to the Commonwealth of Massachusetts transportation agencies.

1.1 Background

Pedestrian infrastructure is one of the most vital transportation infrastructures for pedestrians and wheelchair users who rely on quality sidewalks to facilitate safe and uninterrupted trips in their everyday lives. To meet the obligations of the Americans with Disabilities Act (ADA) Transition Plan and to make informed investment decisions in transportation asset management, MassDOT is responsible for the timely identification and maintenance of inadequate sidewalks in its jurisdiction. It is actively seeking to improve data on existing pedestrian infrastructure to more clearly understand the needs for maintenance and construction of pedestrian facilities. It is MassDOT’s policy to provide equitable accommodation for all modes of transportation that seek conveyance within the Commonwealth. MassDOT’s consistent annual investment in sidewalks and pedestrian “curb cuts” is a clear example of their policies in action.

Another major MassDOT strategic goal is to ensure that investment strategies are founded upon clear performance outcomes. For this purpose, MassDOT maintains high-quality data on bridges and pavement surfaces. This data is used to manage current conditions, develop future performance targets, and support investment models for the preservation and improvement of current and future asset performance. Given their importance to the public, bridges, and roads are valuable transportation infrastructure assets, and considerable annual investments are made to support inspection, processing, and analysis of information about them.

Dedicated resources responsible for pedestrian infrastructure inventory and condition assessment do not currently exist at MassDOT. As a result, current infrastructure data is not of a quality or level of detail from which the organization could make informed investment decisions. A current sidewalk inventory dataset resides within the geographic information system (GIS)-based Road Inventory File (RIF), which is managed by the MassDOT Office of Transportation Planning (OTP). However, there are two major drawbacks of the current dataset due to the labor-intensive and cost-prohibitive manual data collection process in the

current practice: the time-intensive nature of updates and the lack of sidewalk condition information .

With the recent advancement of remote sensing technologies, many mobile systems with high data acquisition frequency and measurement accuracy, including mobile light detection and ranging (LiDAR), have become cost-friendly, and commercially available. The data derived from these mobile LiDAR systems had the potential to address the challenges mentioned above and deliver a comprehensive pedestrian infrastructure inventory database accurately and efficiently. Therefore, while there is an ongoing need for MassDOT to explore and implement a cost-effective, efficient, and reliable means to inventory its pedestrian infrastructure, there also is an emerging need for MassDOT to leverage the advancement of the new technologies and the availability of the emerging data to address the former.

1.2 Objectives and Detailed Work Tasks

This research project seeks to demonstrate the feasibility of mobile LiDAR as a viable technology to support efficient inventory update and condition assessment of the pedestrian infrastructure at MassDOT. With embedded geolocation and geometric measurement information, the derived database from the mobile LiDAR can be seamlessly integrated with the existing RIF managed by MassDOT. It is expected that the pedestrian infrastructure data will provide the Highway Division with accurate information from which to prioritize sidewalk maintenance needs. Focusing on the State Route 9 corridor, the objective of this research project is to collect and process data with a mobile LiDAR system, to verify and update the existing MassDOT's sidewalk inventory data, and to incorporate condition information into the inventory geodatabase. The detailed work tasks are listed as follows:

- Task 1 - Review of Pedestrian Infrastructure Inventory Efforts: The research team conducted a detailed literature review on available and ongoing research and implementation efforts for pedestrian infrastructure inventory and condition evaluation that have been made by MassDOT, other transportation agencies, and the research community. The research team also worked with OTP to obtain the available pedestrian infrastructure data that is currently residing within the GIS-based RIF.
- Task 2 – Mobile LiDAR Data Acquisition: The research team conducted a comprehensive data acquisition task using the mobile LiDAR sensor (i.e., Riegl VMZ-2000) along the State Route 9, covering 271.76 miles in both bounds. Three full data acquisition sessions were included to ensure the data coverage and repeatability, while two additional testing data acquisition sessions were included for determining the optimal sensor configurations.
- Task 3 – LiDAR Data Processing for Pedestrian Infrastructure Inventory/Update: The research team developed computer-aided LiDAR processing algorithms and interactive

point cloud processing tools for identifying the locations and geometries of the critical pedestrian infrastructures along State Route 9 in both bounds. Complete sidewalk inventory results were derived and then compared with the existing sidewalk inventory database provided by MassDOT. The research team evaluated the completeness and accuracy of the existing inventory and then updated the current pedestrian infrastructure inventory database with the new LiDAR-based results. As the current sidewalk inventory database does not contain entries for curb ramp inventory, the research team created a new geodatabase for referencing these pedestrian infrastructures separately. The research team evaluated the overall processing time for completing the inventory update using mobile LiDAR data.

- Task 4 – LiDAR Data Processing for Pedestrian Infrastructure Condition Extraction: The research team developed computer-aided LiDAR processing algorithms and interactive point cloud data processing tools for extracting the condition information that corresponds to the inventoried pedestrian infrastructure on State Route 9, including cross slope and grade for sidewalks and the running ramp slope for curb ramps. The research team also evaluated the overall processing time for completing the condition extraction using mobile LiDAR data.
- Task 5 – New Pedestrian Infrastructure Geodatabase/Schema Development: The research team worked with MassDOT OTP to develop a new pedestrian infrastructure inventory geodatabase, based on the existing PedFcIty database, that can be integrated with the current GIS-based RIF and can host both the essential inventory information and the newly identified condition information. The derived results from State Route 9 were populated into the new geodatabase as a demonstration.
- Task 6 – Reporting of Results: The final report consists of a summary of all research efforts, including suggestions for a successful implementation of a network-level sidewalk inventory and condition evaluation using mobile LiDAR data.

1.3 Organization of this Report

This report is organized as follows. Chapter 1 introduces the background, research needs, objectives, and the detailed work tasks of this research project. Chapter 2 presents the proposed method, including the literature review, the developed algorithms for processing mobile LiDAR data, and the interactive tool. Chapter 3 presents the results of the proposed method. Chapter 4 summarizes the findings and results of this project and recommendations for future studies.

This page left blank intentionally.

2 Research Methodology

The research methodology for this study consisted of three main parts: a review of existing data and technologies, collection of the mobile LiDAR data, and the processing of the mobile LiDAR data for pedestrian infrastructure inventory. Section 2.1 presents a review of the literature related to the existing effort for sidewalk inventory and the existing sidewalk data at MassDOT. Section 2.2 presents an overview of the research methodology, followed by Sections 2.3 through 2.6 that describe the methods for mobile LiDAR data acquisition and processing for generating pedestrian infrastructure information, including sidewalk inventory and measurements as well as curb ramp inventory and measurements.

2.1 Literature Review

2.1.1 Existing Efforts of Sidewalk Inventory

In 1990, ADA developed a set of standards and guidelines for implementing environmental facilitators with the intention of enabling the accessibility of “the public street to people with disabilities with a continuous, unobstructed pedestrian circulation network to the maximum extent feasible.” The Americans with Disabilities Act Application Guideline (ADAAG) specifies a series of critical features for designing and constructing sidewalks that allow uninterrupted and safe trips for wheelchair users. State and local transportation agencies are required to assess the infrastructure’s regulatory compliance with ADA and are responsible for the timely maintenance of any inadequate sidewalks under their care. Although it is usually impractical for transportation agencies to comprehensively carry out these activities promptly due to the labor-intensive and cost-prohibitive nature of the manual data collection process involved with current practices, many of these transportation agencies have attempted to develop sidewalk and curb ramp inventories using both manual and automatic methods.

The research team has identified a total of 17 transportation agencies and communities that have successfully implemented their sidewalk inventories, including one state agency, the state of New Jersey (New Jersey Department of Transportation, 2007); three county/regional agencies, the counties of Franklin, Delaware, Fairfield and Licking in Ohio (Ohio Department of Transportation, 2018), the County of Delaware, Pennsylvania (Planning Department, 2018) and the County of Boone, Missouri (MID-MO Regional Planning Commission, 2014); and thirteen city agencies: the City of Tucson, Arizona (Cole and Leon, 2012), the City of Bellevue, Washington (Loewenherz, 2010), the City of Urbana-Champaign, Illinois (Department of Transportation, 2016), the City of Boston, Massachusetts (Boston Public Works Department, 2015), the City of Toronto, Canada (City of Toronto, 2015), the City of Lee’s Summit, Missouri (Burns & McDonnell Engineering Company, 2009), the City of Texarkana, Texas

(Data Transfer Solutions, LLC, 2017), the City of Ironton, Ohio (Mannik & Smith Group, Inc, 2018), the City of Columbia, Missouri (Public Works Department, 2018), the City of Lakewood, Colorado (Hometown Colorado Initiative, 2015), the City of Los Angeles, California (Gooch, 2017), the City of San Diego, California (Street Division, City of San Diego, 2015), and the City of Rutland, Vermont (Department of Public Works, 2013).

Through the review of these implemented inventories, the following findings were identified from the perspectives of the inventory coverage, the employed technology, the information included in the inventory, and the cost and productivity of the projects.

- **Coverage**: The effort on inventorying pedestrian infrastructures has been a continuously ongoing process by public agencies and communities. Some of the earliest efforts can be traced back to more than a decade, such as at the New Jersey Department of Transportation (NJDOT) (New Jersey Department of Transportation, 2007) and in Bellevue, Washington (Loewenherz 2010), but most of the inventories have only concluded recently. However, only NJDOT, out of the 17 implemented inventories, covers an extensive length of the network on a state level, while the rest of the inventories only covered a very small region and network within the city's or county's jurisdictions. While the financial burden partially constrains a broader implementation, the limitation of the existing technologies plays a more significant role.
- **Technology**: The advancement of inventory technologies has played an essential role in successful implementations. From a data acquisition perspective, GPS- and camera-equipped handheld computers have been widely utilized to inventory the existing sidewalk infrastructure. To improve the productivity of the data acquisition, integrated mobile systems, e.g., Ultra-Light Inertial Profiler (ULIP), were introduced (Loewenherz, 2010), and inventory efforts were conducted with the recurrent highway pavement performance survey (Data Transfer Solutions, LLC, 2017; New Jersey Department of Transportation, 2007). However, most data acquisition efforts are conducted manually, e.g., a walking survey. From a data processing and integration perspective, GIS technologies have been broadly utilized, so sidewalk inventories can be conveniently integrated and easily shared with the public, such as in the City of Toronto (City of Toronto, 2015) and the City of San Diego (Street Division, City of San Diego, 2015). However, most of the current data processing efforts remain manual, especially when it comes to detailed condition properties of sidewalks or ramps (Loewenherz 2010). Other applications of emerging technologies, e.g., aerial orthophotos (Department of Public Works, 2013), were developed with promising results that led to successful implementation. However, none of the transportation agencies or communities have attempted the LiDAR-based method.
- **Inventoried Information**: A complete sidewalk inventory covers the primary pedestrian infrastructure of sidewalks and curb ramps with both their locations and conditions (Ai and Tsai, 2016b). However, most of the implemented inventories focus primarily on the locations of the sidewalks. Only a few inventories contain the locations of curb ramps or

the conditions of the sidewalks and curb ramps. The inventories in Tucson, Arizona (Cole and Leon, 2012), Bellevue, Washington (Loewenherz 2010), and Urbana-Champaign, Illinois (Department of Transportation 2016) contain the most comprehensive information. It should be noted that due to the limitation of the technologies employed in the data acquisition and processing, and the constraints of project budgets, these inventories were conducted in multiple stages. The conditions and locations for the sidewalks were progressively implemented, as were the locations and conditions of the curb ramps.

- **Cost and Productivity:** The research team identified most of the projects were concluded within two years, thanks to the smaller coverage of the inventoried network. However, due to the different levels of details in various projects, the labor hours for different implementations varied significantly. The research team only identified limited information about the cost of these successful inventories. Despite the employed technologies in these implementations, the project costs tended to increase significantly if additional information was included. For example, the City of Bellevue, Washington, and Lee's Summit, Missouri inventoried similar network lengths of sidewalks, but the City of Bellevue spent over \$100,000 more (more than 30% of the total cost) than the City of Lee's Summit for an additional 4,586 curb ramp locations (Burns & McDonnell Engineering Company, 2009).

2.1.2 Technologies and Methods for Sidewalk Inventory

While many sidewalk inventories have been successfully implemented by local and state transportation agencies, the research team identified the implementation of the coverage, the accuracy, the comprehensiveness of the inventoried information, and the productivity of these inventories were constrained by the limited applications of the emerging technologies and the lack of automated or semi-automated methods. With the recent advancement of remote sensing technologies, many mobile systems with high data acquisition frequency and measurement accuracy (e.g., video log imagery, mobile LiDAR) have become cost-friendly and commercially available—with better data quality. In recent years, there have been many existing studies on developing automated or semi-automated sidewalk extraction and measurement methods by taking advantage of these emerging remote sensing technologies.

The early studies mainly focused on images coupled with GPS positioning mechanisms. Most of these studies dealt with the localization of pedestrian infrastructures. A broad spectrum of imagery was attempted to balance the coverage of the network with the granularity of the sidewalk data, including aerial imagery, video log imagery, crowdsourcing imagery, etc. Guo et al. (2004) segmented the road areas in aerial imagery by matching digital line graph (DLG) maps, and sidewalk edge detection was subsequently employed based on the preliminary segmented results. A few more recent studies continue with a similar pipeline by Guo et al. (2010). However, due to the limited resolution of the imagery, it was less feasible to extract the curb ramp conditions and locations using an image-based method. Hara et al. (2013, 2014)

developed a support vector machine (SVM)-based computer vision technology to identify the presence of curb ramps using Google Street viewer images. The histogram of the Gaussian feature was employed as the primary feature associated with curve ramps. A semi-automated interface was also developed to facilitate the manual process in case the automated algorithm failed. Ai and Tsai (2016b) developed a deformable part model (DPM) that used high-resolution video log images to identify the accuracy boundary of the curb ramps. Although the existing image-based sidewalk and curb ramp extraction algorithms have shown promising results, the major drawbacks of the image-based method (e.g., a lack of accurate geometry measure) prevent these methods from evaluating the geometry of the sidewalk and curb ramps.

With the emergence of new connected and autonomous vehicles, mobile LiDAR data, and other depth-enabled data have become widely available. Most of the recent studies have focused on LiDAR-based methods. These methods efficiently identify the locations of sidewalks and curb ramps. They also accurately evaluate the geometry and condition of these infrastructures. However, limited numbers of studies have focused on sidewalk extraction or inventory. In this technical memo, the research team further investigated three studies for pedestrian infrastructure identification and evaluation in detail to assess the state-of-art performance of these methods, and to reveal the potential applications of LiDAR-based methods. Each of these three methods is representative of the state-of-art LiDAR processing techniques, namely the geometry-based method, the reflectance-based method, and the scan-based method, which have shown promising results for sidewalk and roadway extraction.

Geometry-based Method

As sidewalks and curb ramps are distinguishable by their unique geometrical shapes (e.g., edge or plane) and geometrical measurements (e.g., length, width, adjacency), the geometry-based segmentation method has been identified as an efficient and accurate approach. Balado et al. (2018) proposed such a new approach to automatically detect and classify five categories of urban ground elements, including roads, sidewalks, treads, risers, and curbs. There are mainly two steps in the methodology, as shown in Figure 1.

- Step 1 focuses on a planar segmentation and refinement to divide point clouds into planar regions. After the initial normal-based segmentation, split and merge operations are followed to reduce segmentation errors caused by the quality of the input data or the disturbance caused by small road objects. Finally, the coplanar refinement and road-sidewalk refinement are applied to fine-tune the identified object based on the coplanar constraint and the normal variance constraint, respectively.
- Step 2 focuses on classifying the planar region into different ground element categories based on empirical geometry constraints. In this classification, four classes (risers and curbs, treads, sidewalks, and high vertical elements) are considered for classifying point

cloud regions according to the geometry constraints, including the horizontal and vertical dimensions and the tilting angles.

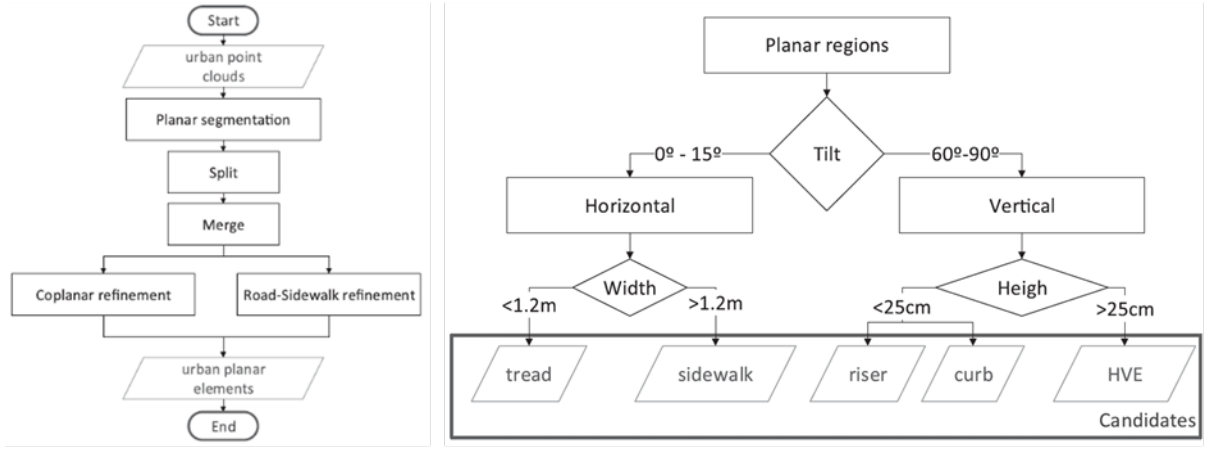


Figure 1 Flowcharts for Steps 1 and 2 of the sidewalk extraction algorithm (Balado et al., 2018)

The final topologic validation step is applied to finalize the process based on the empirical ground object adjacency. All the classification results and their spatial relations are stored in a graph library that is scalable to larger datasets. The methodology was tested in four real-world datasets, and the results show a correct classification rate of 97.0%. However, researchers noticed that the proposed method shows better results for larger elements (e.g., sidewalks, roads, etc.), while underperforms for smaller elements (e.g., curbs, treads, risers, etc.). This is primarily attributed to the more distinguishable coplanar geometry in larger elements, and, in addition, attributed to the more points associated with, the larger elements that reveal more distinguishable geometry constraints.

Reflectance-based Method

Besides the unique geometrical shape and adjacent constraints, many of the road objects, e.g., pavement marking (Soilán et al., 2018) and signage (Ai and Tsai, 2016a), are also distinguishable because of their unique features captured by LiDAR, such as reflectance intensity. Soilán et al. (2018) proposed a method for the detection of road and sidewalk networks by taking advantage of the unique reflectance feature. The urban ground-level, semantic information (e.g., road edges, sidewalks) can be identified efficiently through the point cloud preprocessing. Figure 2 shows the overall flow of the proposed algorithm, consisting of five primary steps, including point cloud preprocessing, elevation-based segmentation, ground extraction, curb map definition, and roadway feature extraction.

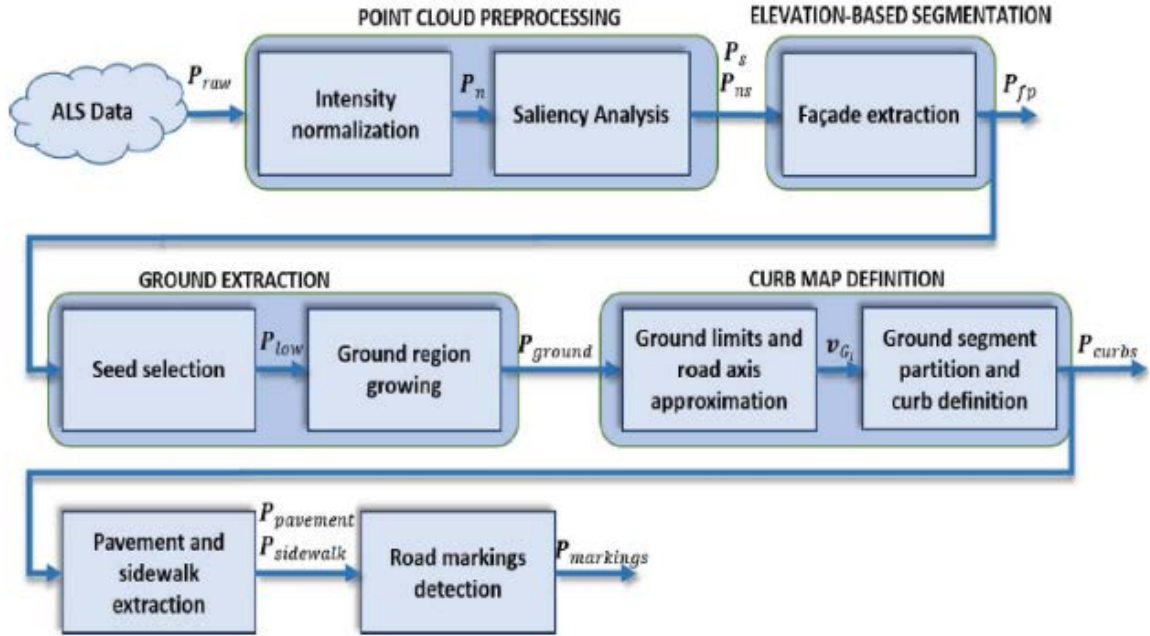


Figure 2 Flowchart of the proposed road feature extraction algorithm (Soilán et al., 2018)

- Step 1 focuses on the preprocessing of the point cloud by normalizing the reflectance intensity based on the laser scanning model, and by creating a saliency map derived through a distance projection. The normalization process takes advantage of the unique physical characteristics of the point cloud reflectance, determined by beam distance and incidence angle, and efficiently homogenizes the points for all road objects. The saliency mapping process is then applied to identify the point clusters whose surfaces only change gradually, such as roofs, balconies, and ground segments, and the point clusters whose surfaces change drastically—façades, poles, lateral sides of vehicles, etc.
- Steps 2-5 follow a similar approach as other geometry-based methods by taking advantage of the geometrical shapes (e.g., edges and planes) and geometrical measurements (e.g., elevations and elevation gradients). It should be noted that although features like reflectance can be used to efficiently extract many road objects that are effective visual cues and spatial references for sidewalks, geometrical shapes and measurements remain critical for extracting sidewalks and other pedestrian infrastructures. Therefore, geometry- and reflection-based methods are usually coupled to produce a better performance regarding accuracy and productivity.

Besides sidewalks, the proposed method is also applied to extract pavement and pavement markings. The results show promising results of F-scores around 95% for pavement as well as sidewalks, determined through a test conducted over a high-density urban LiDAR data set for

a portion of Dublin, Ireland. However, the computation efficiency remains a challenge due to the employed complex façades extraction and ground region-growing methods.

Scan-based Method

While most of the existing LiDAR-based methods focus on the combination of geometry and reflectance features for more accurate and efficient road object extraction, one of the critical features is often overlooked: the scanning pattern. If this piece of crucial information is known beforehand, which is usually the case, accuracy and productivity can be significantly improved. Ai and Tsai (2016b) proposed a method for sidewalk extraction by taking advantage of the linear scanning pattern of the collected data using a line-scanning LiDAR. Instead of treating the LiDAR point cloud as an arbitrary cluster, the proposed method treated the linear scanning pattern as a continuous sequence with linkage information. Therefore, instead of a 3-D segmenting for all the points, a much simpler 2-D segmentation for each scan that is perpendicular to the traveling direction is applied. Figure 3 shows the scan pattern and the detail of the segmentation of a scan line.

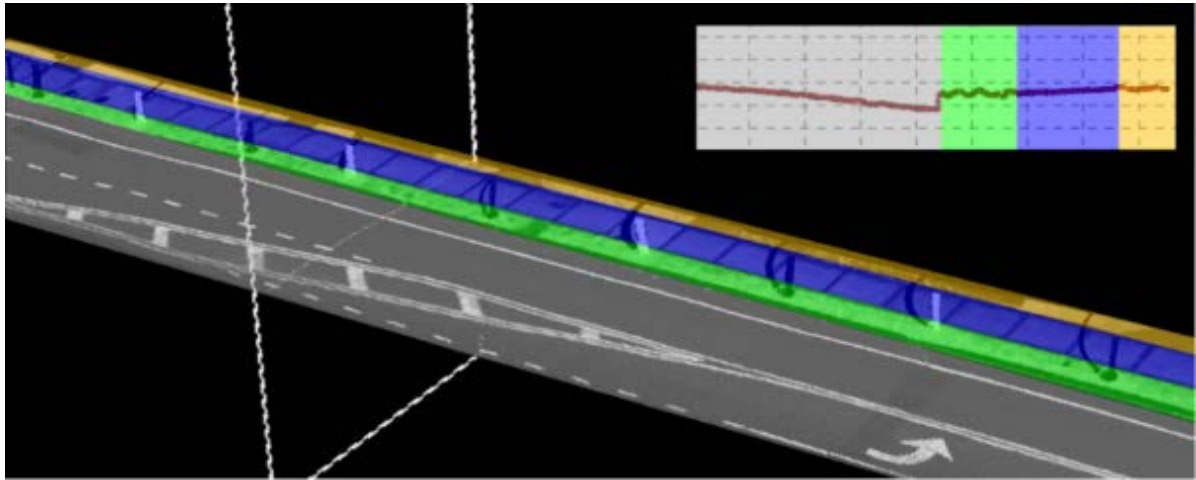


Figure 3 Illustration of the 2-D LiDAR scan-based segmentation algorithm (Ai and Tsai, 2016b)

Although a 2-D segmentation works effectively with better efficiency than a 3-D segmentation, a strong assumption that an ideal roadway cross-section comprised of four zones, including driveway zone (gray), planter zone (green), pedestrian zone (blue), and frontage zone (yellow) must be made when using this approach. Such an assumption does not often hold due to the presence of a parked vehicle, interruption of the sidewalk (such as an intersection), or other interfering objects (e.g., tree trunk, fire hydrant). Therefore, a segmentation connection method can be introduced to adjust the segmentation results and to link results from consecutive scans into a continuous boundary. Figure 4(a) illustrates the original segmentation results in successive scans, where the dash lines represent the laser scans, and red dots represent the raw

segmentation results. The segmentation results are clustered longitudinally based on the k-nearest neighbor (k-NN) method. Figure 4(b) illustrates the clustered results, where different circles represent the label of the clusters. The spatial relationship in the longitudinal direction is then measured to further merge the clusters that are along the same trace in the longitudinal direction, as shown in Figure 4(c). The spatial relationship in the transverse direction is measured to remove the collinear segments with a shorter length. Figure 4(d) illustrates the results after the removal of the red cluster. A B-spline algorithm is then introduced to connect different segmentation points smoothly. Figure 4(e) shows the results of the final segmentation results, where different colors represent the corresponding zones of the driveway (gray), planter (green), a pedestrian (blue), and frontage (yellow).

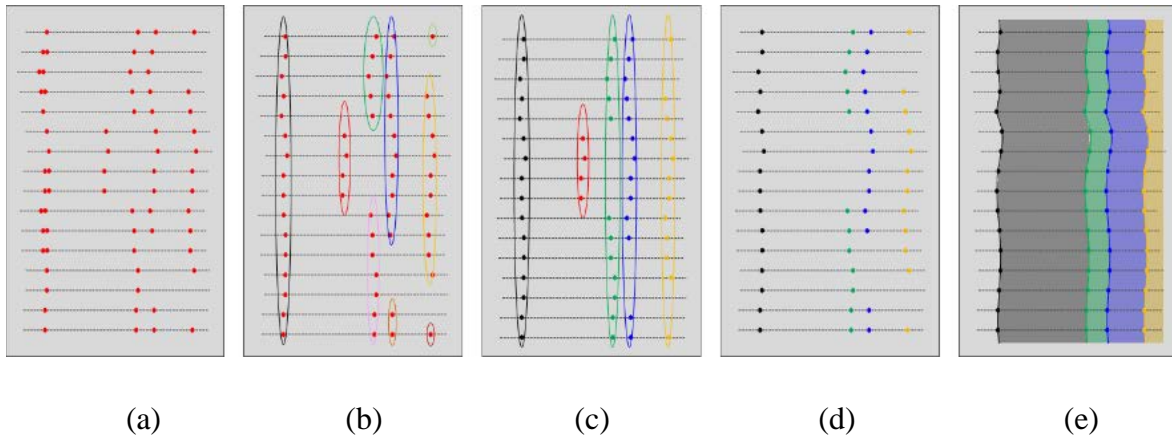


Figure 4 The process of the cross-section segmentation connection method (Ai and Tsai, 2016b)

The results show that out of the two-mile tested sections, more than 98.3% of sidewalks can be successfully identified with minimal false detection (defined as excessive obstructions by utility facilities and shuttle buses). More importantly, the processing time for extracting the sidewalk using the 2-D method is significantly faster than the traditional 3-D segmentation method using both geometry and reflectance features. Beside sidewalk extraction, the proposed study would also develop a data fusion technique for integrating the video log images with the mobile LiDAR data. The image-based method using DPM for curb ramp identification can effectively project its results to the LiDAR point cloud; therefore, the corresponding slope measurements can be conducted subsequently for ADA compliance.

Summary

Although LiDAR-based methods are applied in many other road object extractions and show promise in sidewalk inventory, only limited numbers of such studies have been identified through this technical review. The existing methods using geometry, reflectance reference, and scanning patterns have been reliable in extracting the locations of sidewalks, and some of them have proven to be efficient in their use of time and resources. However, there remains room for performance improvements for these methods in regard to both accuracy and productivity.

- For the scope of sidewalk extraction, while Ai and Tsai (2016b) have developed a method with considerable accuracy and efficiency, their method remains to be validated with a larger dataset, and the strong assumption of the scanning pattern needs to be improved for a more practical application. Therefore, the research team carried out the work task of sidewalk extraction based on the method proposed by Ai and Tsai and made critical improvements to address the technical challenges that may hinder this method from large-scale implementation, including 1) it relies on strong priors, e.g., sensor configuration and scene context to tune the parameters for consistent results; 2) it can only handle simple scenes where features of interest are significant; 3) it relies on an iterative and sequential search and match strategy for sidewalk extraction that can be time-consuming and infeasible for large-scale data sets.
- For the scope of curb ramp extraction and condition evaluation, while a few studies have focused on curb ramp identification using image processing and crowdsourcing (Hara et al., 2013 and 2014), the research team only identified Ai and Tsai's method (2016b) as being capable of both extracting the curb ramp locations and measuring their critical slope information. Therefore, the research team carried out the work task of curb ramp extraction by directly adopting the method proposed by Ai and Tsai.

2.1.3 Current Efforts of Sidewalk Inventory in MassDOT

MassDOT actively collects roadway inventory data and maintains a centralized geodatabase (the RIF) to facilitate data consolidation, data processing, data visualization, and data sharing. The existing sidewalk inventory data resides in the RIF, including the location of the sidewalk, curb type, left and right sidewalk width, pedestrian surface type, and pedestrian facility type. MassDOT has also developed and maintained a separate geodatabase called CurbRamp to facilitate the data integration that is dedicated for curb ramp facilities. The existing curb ramp inventory data include the curb ramp location, inspection results (missing components), inspection comments, current status, visual deficiency, and other factors. Figure 5 shows a screenshot of the RIF data fields with the highlight of the corresponding sidewalk infrastructure information (in brown) and the CurbRamp data fields (in blue).

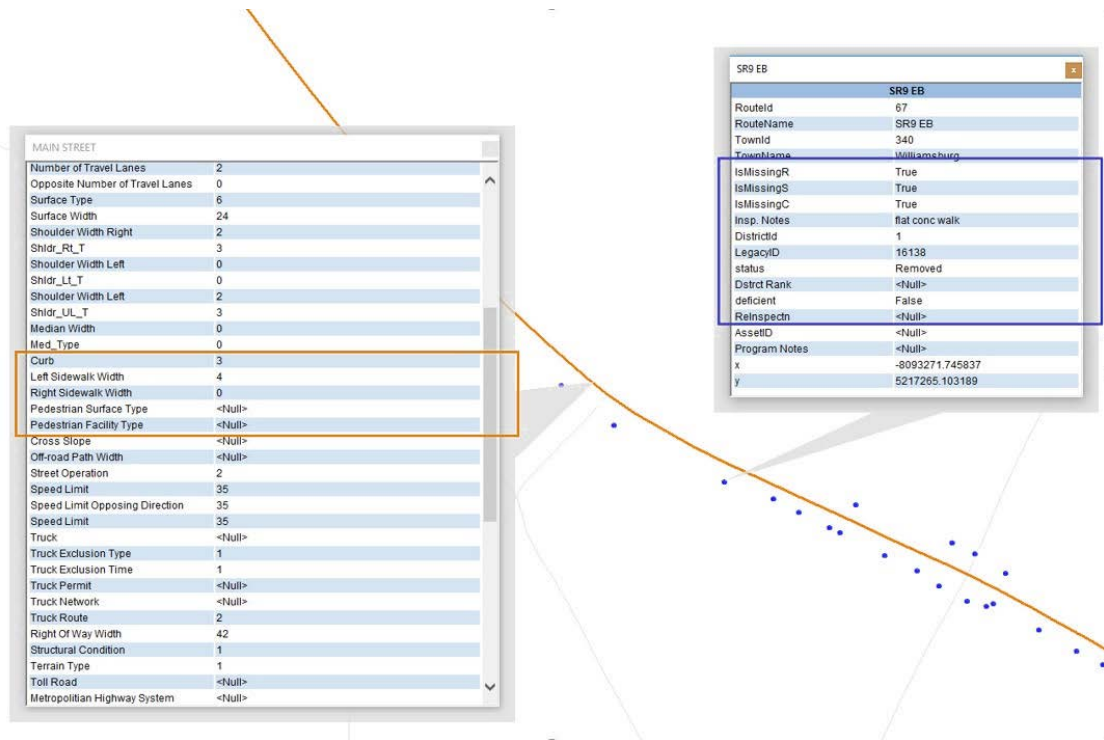


Figure 5 A screenshot of the RIF data field (in brown) and the Curb Ramp data fields (in blue)

MassDOT has made an effort to inventory the sidewalks and curb ramps in its network and has developed a comprehensive data structure to house and analyze the information (the geodatabases of RIF and CurbRamp). However, the following limitations have been identified by the research team:

- **Sidewalk location:** The current sidewalk inventory is conducted based on the Road Segment ID stored in the RIF. While it is convenient to maintain and reference the existing highway performance management system (HPMS) and the pavement management system, the delineation of the sidewalks may not align well with the delineation of the Road Segment.
- **Sidewalk condition:** While the data fields for sidewalk conditions include the sidewalk width measurements, other important geometries (including sidewalk grade, sidewalk cross slope, etc.) have not been included. Also, as the sidewalk widths were estimated based on the manual inspection and the orthograph imagery analysis, the accuracy remains to be validated.
- **Curb ramp location:** The current curb ramp inventory has been spatially referenced based on the curb ramps' XY coordinates. While the relative coordinates concerning the road inventory are all populated in the map (as shown in Figure 5), the locations and existence of these inventory ramps remain to be validated.

- Curb ramp condition: While the data fields for curb ramp condition include inspection results conducted by the field engineers, they only include whether the curb ramp misses any component, and whether the curb ramp is currently active or not. Some of the critical geometrical information is missing, such as the curb ramp slope.

Focusing on State Route 9 in this research project and based on the collection of the existing pedestrian infrastructure data from MassDOT, the research team aims at addressing the limitations mentioned above using the LiDAR-based method. It is expected that the LiDAR-based method will be able to accurately validate the existing inventory locations for the sidewalks and curb ramps and to populate the corresponding condition information efficiently. Figure 6 shows the overview of the scoped region with the highlighted road sections from the RIF geodatabase (in red) and the inventory curb ramps from the CurbRamp geodatabase (in green).

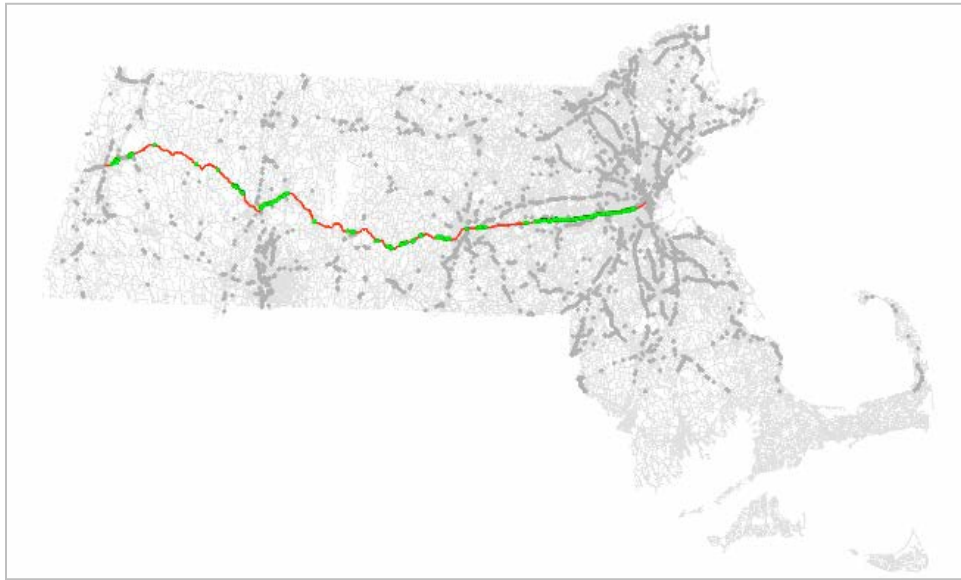


Figure 6 Illustration of the SR9 corridor of interest for this research project

2.2 Methodology Overview

In this study, the research developed a complete data processing methodology for sidewalk inventory and curb ramp condition evaluation from the raw LiDAR data acquisition to GIS integration. This methodology consists of six key steps, including Data Acquisition, Point Cloud Segmentation, Sidewalk Extraction, Curb Ramp Extraction, Key Feature Measurement, and the final Sidewalk Inventory. Figure 7 shows an overview of the research methodology. The subsequent sections present the detailed methods and algorithms developed in this study for each key step of this complete data processing methodology.

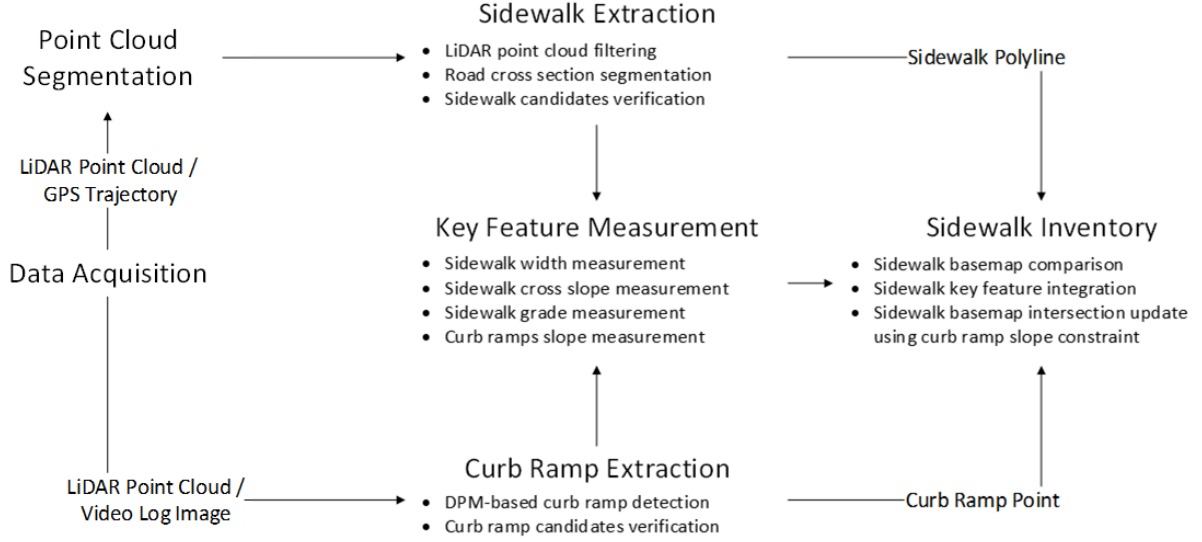


Figure 7 Overview of the research methodology

2.3 Data Acquisition

The data acquisition system used in this study is an integrated mobile LiDAR system, RIEGL VMZ-2000, that consists of three primary components: the LiDAR sensor, the precise positioning system, and the camera system. The LiDAR sensor is used to acquire the point cloud of the roadway, including pedestrian infrastructures. Each point consists of the precise position information that is derived from the integrated precise positioning system. The integrated precise positioning system is used to acquire accurate coordinates that are composed of a global positioning system (GPS) and an inertial measurement unit (IMU). The camera system is used to capture video log images that are registered to the LiDAR sensor. In this study, the point cloud data acquired by the LiDAR sensor was used for the subsequent processing, while the precise positioning system and the camera system were used for positional correction and visual reference for the point cloud, respectively.

The current LiDAR sensor can produce 400,000 measurements per second in both line-scanning mode and radar-scanning mode. For the application of the corridor scanning with the best point cloud density, the line-scanning mode was selected. Figure 8 shows the vertical and horizontal configurations for the line-scanning mode.

- For the vertical configuration, the scanning line of the LiDAR sensor is aligned perpendicular to the ground when the vehicle makes a longitudinal motion. The scanning line forms a 100° vertical fan to cover the road surface, especially the roadside objects. To acquire the point cloud with better homogeneity of point cloud densities, the frequency of

the LiDAR sensor and the LiDAR heading angle were configured at 75 Hz (i.e., lines per second) and 135° (i.e., the angle to the vehicle driving direction), respectively.

- For the horizontal configuration, the scanning line of the LiDAR sensor is aligned parallel to the ground when the vehicle makes a longitudinal motion. The scanning line forms a 100° horizontal fan to cover the road surface at the back of the vehicle. To balance the density and the coverage of the point cloud, the frequency of the LiDAR sensor and the LiDAR pitching angle were configured at 75 Hz (i.e., lines per second) and -15° (i.e., the angle to the level of the vehicle), respectively.



Figure 8 Mobile LiDAR installations for both vertical and horizontal configuration

With different trials of configuration, the vertical configuration was selected for better point cloud density that is associated with the roadside features. In this study, the radar mode was not evaluated in detail due to the now-known fact of inhomogeneous point cloud density, because the radar mode is primarily designed for stop-and-go operations.

2.4 Point Cloud Segmentation

The objective of point cloud segmentation is to decompose the large-scale, raw point cloud data into feature-rich, meaningful groups so that the subsequent sidewalk extraction algorithms can be applied efficiently. Previous research has been done for segmenting LiDAR point cloud with high accuracy using deep learning. Liu et al. (2017) introduced a deep reinforcement learning method to parse the large-scale 3D point clouds and map the raw data to make the classification. Maturana et al. (2015) used VoxNet, a supervised convolutional neural network (CNN) integrating a volumetric grid, to realize the robust object recognition. However, most neural networks do not directly consume the raw point clouds but require preparation, such as voxelization, which can be ineffective. PointNet (Charles et al., 2017) is a pioneering CNN that directly processes the raw point clouds, which reflects the permutation invariance of the inputting points. PointNet has increasingly been applied to object classification and semantic segmentation thanks to its high efficiency. There are two steps in the formulation of PointNet: the spatial encoding of every point is obtained first, and then all individual point features are

aggregated to a global point cloud signature. Although PointNet is an efficient and effective neural network, it cannot capture the local structures which limit PointNet from complex scenes. The hierarchical neural network, PointNet++ (Qi et al., 2017), as an extension of PointNet, was introduced to solve this problem. It applies PointNet recursively on a nested partitioning of the input point set. PointNet++ can achieve both the robustness under density variation and a high level of detail captured in the local feature. However, very few efforts have been made to apply PointNet++ to road scene segmentation. Therefore, this study introduces PointNet and PointNet++ for efficient point cloud segmentation.

In this subsection, the algorithms for both PointNet and PointNet++ are briefly described, followed by the customized training process used by the research team.

2.4.1 PointNet

PointNet directly processes the input point clouds without transforming to other data structures, such as voxel or graph, and outputs each point segmentation label corresponding to the input per point. This network architecture maintains three properties of the input point clouds: it is unordered, displays interaction among points, and shows invariance under transformations. PointNet can be used in many tasks, such as 3D shape classification, shape part segmentation, and scene semantic segmentation. This component of PointNet mainly concentrates on scene semantic segmentation.

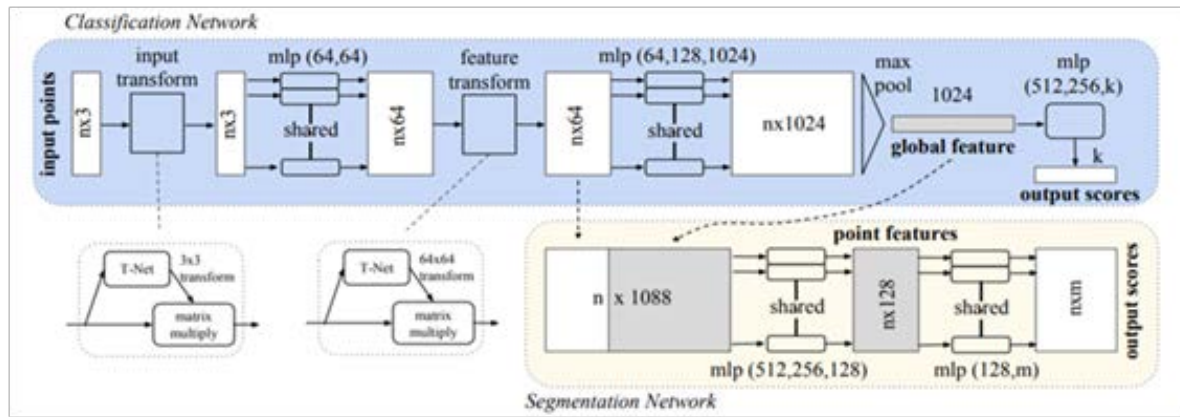


Figure 9 PointNet Architecture

The network architecture of PointNet is shown in Figure 9. There are three key modules in PointNet architecture: symmetry function, local and global information aggregation structure, and joint alignment network. The symmetry function embedded in the max-pooling layer aggregates the information of the input points for unordered input. The local and global information aggregation structure is used for the point segmentation with high effectivity. Both the input points and point features are aligned by two joint alignment networks.

In order to make an invariant permutation for the input points, a simple symmetry function is used to aggregate the information of the input data. The function is defined via a point set by transforming elements in the set.

$$f(\{x_1, \dots, x_n\}) \approx g(h(x_1), \dots, h(x_n))$$

Where $f: 2^{R^N} \rightarrow R$, $h: R^N \rightarrow R^K$ and $g: R^K \times \dots \times R^K \rightarrow R$ is a symmetry function with n R^K s multiplications. h is approximated by a multi-layer perceptron network. g is approximated by a composition of a single variable function and a max-pooling function.

The combination of local and global information is achieved by this structure for the point segmentation (as shown in Figure 9). The global features are fed back to each point feature by concatenating the global feature with per-point features. The new per-point features are extracted based on the combined point features generated in the above step. At the same time, the per point feature contains local and global information.

A joint alignment network keeps the point set invariant while undergoing geomatic transformations. A mini-network (T-net, as shown in Figure 9), which resembles the big networks, is used to predict an affine transformation matrix. The network directly applies this transformation to the coordinates of input points. Another alignment network is also applied in the alignment of the feature space with the help of adding a regularization term to the softmax training loss. A feature transformation matrix can be predicted by this network to align the features from different input point clouds.

2.4.2 PointNet++

The hierarchical neural network PointNet++ was introduced since PointNet cannot capture the local features introduced by the metric. PointNet++ is an extension of PointNet with the same hierarchical structure. Two issues are solved by this neural network: the need to generate the partitioning of the point set and to abstract the local features or point sets through a local feature learner. The farthest point sampling (FPS) algorithm is applied to generate the partitioning of a point set. PointNet++ is used to abstract the sets of the local points or features in a nested partitioning of the point set.

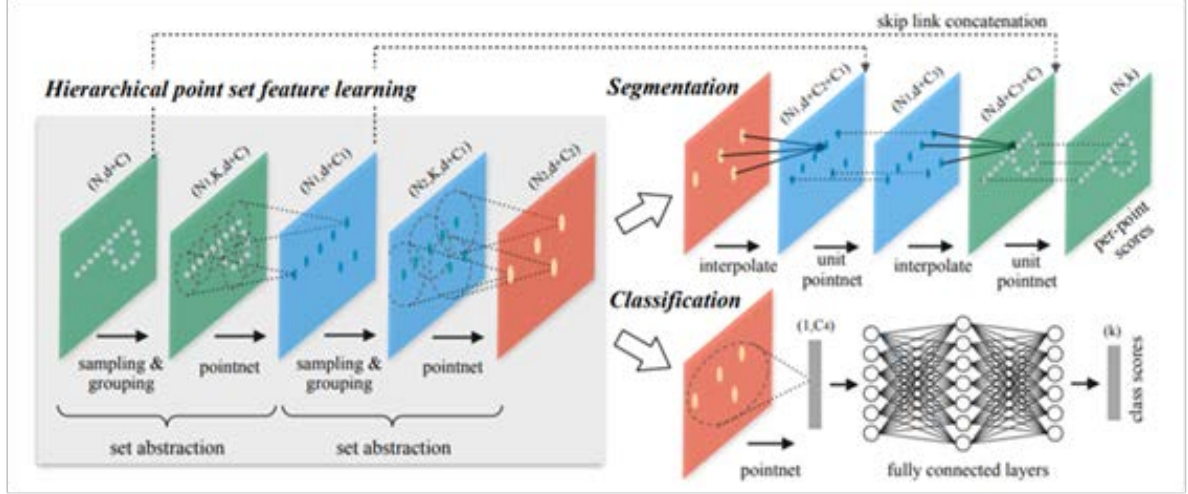


Figure 10 PointNet++ Architecture (Qi et al., 2017)

PointNet++ architecture is visualized in Figure 10. There are mainly two applications: classification and set segmentation. The second application is discussed in this subsection as the relevant background. The hierarchical structure is made of several set abstraction levels. Each set abstraction level contains a Sampling layer, a Grouping layer, and a PointNet layer.

The input $N \times (d + C)$ matrix from N points with $d - \dim$ coordinates and $C - \dim$ point feature is processed and an $N' \times (d + C')$ matrix of N' subsampled points with $d - \dim$ coordinates and $C' - \dim$ point feature summarizing local context is outputted in a set abstraction level.

In the Sampling layer, a set of points defining the centroids of local regions from the input points are selected by using FPS, which has better coverage of the whole point set. A subset of points $\{x_{i_1}, x_{i_2}, \dots, x_{i_m}\}$ is chosen from the input points $\{x_1, x_2, \dots, x_n\}$, where x_{i_j} is the most distant point (in the metric distance) from the point set $\{x_{i_1}, x_{i_2}, \dots, x_{i_{j-1}}\}$ with regard to the rest of the points.

In the Grouping layer, a point set with size $N \times (d + C)$ and the coordinates of the centroids with size $N' \times d$ are inputted. The local region sets are generated by finding the points in the neighbor area of the centroids based on the ball query, which is preferred for semantic point labeling. The groups of point sets with size $N' \times K \times (d + C)$ (K is the number of points around the centroid points) are outputted. Each group matches a local region in this layer.

In the PointNet layer, the size of the input points in local regions is $N' \times K \times (d + C)$. The local regions are abstracted by encoding local region patterns into feature vectors using a mini-PointNet. The size of the output points is $N' \times (d + C')$.

Two types of grouping under non-uniform sampling density when combining features in different scales were proposed: multi-scale grouping (MSG) and multi-resolution grouping (MRG). As shown in Figure 11(a), features at different scales are concatenated to form a multi-scale feature in MSG. MRG is introduced since MSG generates expensive computation for each centroid point at large scale neighborhoods. In MRG (as shown in Figure 11(b)), a region features at some level L_i is a concatenation of two vectors. Summarizing the features at each subregion from the lower level L_{i-1} obtains one MSG (left) by the set abstraction level. Processing the raw points in the local region obtains the other (right) by a local PointNet. The weights of the two vectors are different in different densities of a local region.

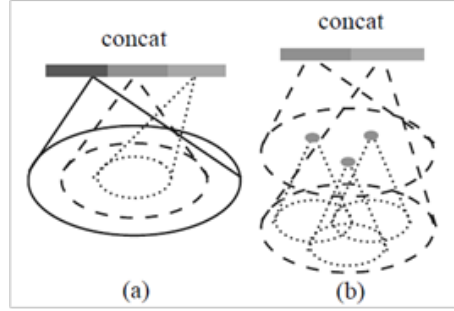


Figure 11 Illustrations of MSG and MRG2 (Qi et al., 2017)

In the set segmentation, the point features of all original points are obtained by propagating the features from the subsampled points to the original points. For point feature propagation, two measures (distance-based interpolation and across-level skip links) are used in the hierarchical structure (as shown in Figure 10). The inverse distance weighted average based on k nearest neighbors is used to interpolate feature values f .

$$f^{(j)}(x) = \frac{\sum_{i=1}^k w_i(x) f_i^{(j)}}{\sum_{i=1}^k w_i(x)}$$

Where $w_i(x) = \frac{1}{d(x, x_i)^p}$, $j = 1, \dots, C$; $p = 2$; $k = 3$.

The interpolated features are concatenated with skip-linked point features from a set abstraction level. The concatenated features then pass through a PointNet unit. Each point's feature is updated by some shared fully connected and Rectified Linear Unit (ReLU) layers. The process is repeated until the features are propagated to the original point sets.

2.4.3 PointNet++ Model Training

In this study, the PointNet++ neural network is trained and validated using the semantic-8 dataset (Hackel et al., 2017), which is popular among researchers. The semantic-8 dataset has

large-scale point clouds with over one billion labeled points for training and validation. The semantic-8 dataset with eight class labels includes 15 scenes (streets, squares, village, etc.). In this study, the improved six classes are used for the road scene segmentation, including man-made and natural terrain (MNT), vegetation including low and high vegetation (V), buildings and structures (BS), hardscape (HS), scanning artifacts (SA), and cars (C). The testing dataset was collected on State Route 9 and manually labeled as six classes according to the semantic-8 dataset for evaluating the trained model. The point clouds of the MNT were obtained by the prediction of the trained model using the unlabeled collected dataset. Figure 12 shows examples of the six classes defined in this study. The basic environment of the road scene segmentation based on PointNet++ is shown in Table 1.

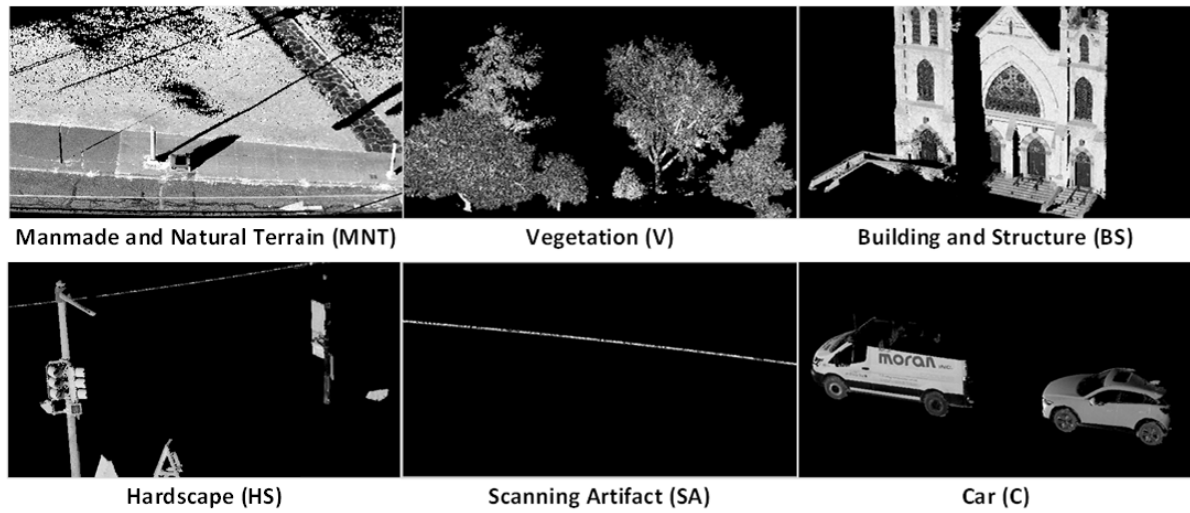


Figure 12 Examples of the six classification classes

Table 1 Basic environment of the road scene segmentation based on PointNet++

Type	Description
Processor	Intel(R) Core (TM) i7-8700 CPU @ 3.20GHz 3.19GHz
Memory (RAM)	32 GB
GPU	NVIDIA GeForce GTX 1080
System type	Ubuntu 18.04 LTS, 64-bit Operating system
Others	TensorFlow 1.8

The datasets “sg27_5”, “sg28_4”, “untermaederbrunnen1,” and “untermaederbrunnen3” in the semantic-8 dataset were used as the validation datasets, and others were used as the training datasets. It required 24 hours, 8 minutes, and 4 seconds to train and validate the model when the epochs were 500. One epoch is a pass through the entire training dataset.

Overall Accuracy (OA) and Intersection over Union (IoU) are used as the metrics. OA is an evaluation metric measuring the detection accuracy. IoU is the ratio between the intersection and the union of two sets (detection result and ground truth). It is calculated based on the following formula.

$$\text{IoU} = \frac{\text{DetectionResult} \cap \text{GroundTruth}}{\text{DetectionResult} \cup \text{GroundTruth}}$$

The detection result is correct if $\text{IoU} \geq 0.5$. IoU will be 1 if the detection result is equal to the ground truth. The changing accuracy, OA, and IoU of each class per epoch are shown in Figure 13. The training model performs at a high accuracy of 94.65% when the epochs are 500, as shown in Figure 13(a). Figure 13(b) depicts that the high IoU 0.53 is obtained in this trained model when the epochs are 500. The training model is stable based on the near-horizontal lines in both Figure 13(a) and (b) when the epoch arrives at 500. The changing IoU of each class per epoch is shown in Figure 13(c). The MNT class performs at a higher IoU of 0.94 when the epochs are 500. The model for training the MNT class also achieves stability with the 500th epoch.

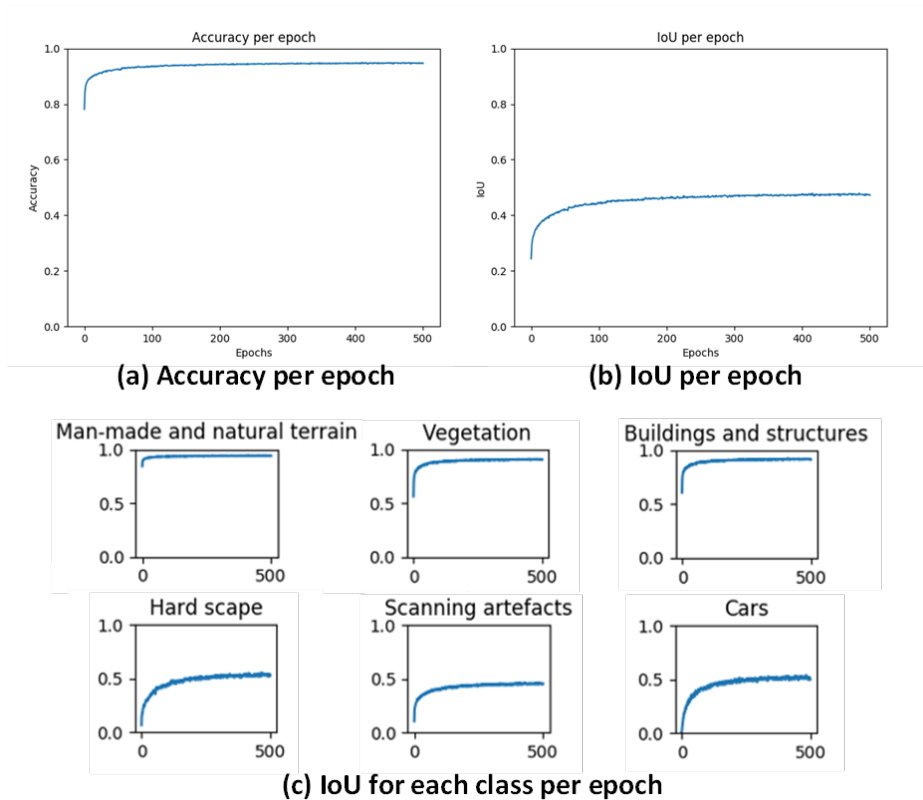


Figure 13 Accuracy, IoU, and IoU of each class per epoch

2.4 Sidewalk Extraction

The objective of this step for sidewalk extraction is to accurately extract the boundaries of the sidewalk from the segmented point cloud that is associated with the man-made and natural terrain. In other words, while many of the existing methods for automated sidewalk extraction using a LiDAR point cloud have shown promising results, the 2-D segmentation method developed by Ai and Tsai (2016b) has shown particularly high levels of efficiency without compromising accuracy. However, due to the limited features that can be used from the 2-D profile, the performance for the regression within each 2-D profile varies and often relies on the post-processing for reconnecting the segmented profile longitudinally. In this study, a stripe-based extraction method is proposed to overcome the challenge 2-D segmentation method encounters. More importantly, the elevation and lateral offset filtering processes that rely on the sensor configuration and the scene context can be effectively removed without impacting the overall performance.

A stripe is defined as the basic processing unit for sidewalk extraction, which covers 3 ft. (approx. 1 meter) of distance along the traveling direction. All the points associated with the man-made and natural terrain class and bounded by a stripe are converted into an octree structure (Vo et al., 2015) and processed in twofold, including:

- **Stripe Splitting:** The split process of the algorithm is to recursively split the point cloud until each node of the octree only contains points that satisfy the coplanar criterion. Figure 14(a)-(c) shows an illustration of the split process using a 2-D example. Figure 14(a) shows space containing all point clouds within the stripe as the root node. Since the coplanar criterion is not satisfied, space is split into eight sub-spaces (only four shown in Figure 14(b)). The points set in nodes 1 and 2 passes the coplanar criterion, so no further split is required. The points set in node 0 will be further split into eight sub-spaces, as shown in Figure 14(c). Since the points set in all the nodes pass the coplanar criterion, no further split is required.
- **Stripe Merging:** The merge process of the algorithm is applied to combine the neighboring nodes if the points in the combined node still satisfy the coplanar criterion. The merging process will be exhaustively conducted until no neighboring nodes can be merged without violating the coplanar criterion. Figure 14(d)-(f) shows an illustration of the merge processing. As shown in Figure 14(d), the points in neighboring nodes can share a similar normal direction, which indicates that these points should be merged into the same cluster. Therefore, for each node, the coplanar test is conducted by including the points from one of the neighboring nodes. If the coplanar criterion is satisfied, the two nodes are merged into one, as shown in Figure 14(e). The merging process is exhaustively conducted for all the nodes until no further merging can be conducted. Figure 14(f) shows the results of the clustering. Two nodes (i.e., two clusters) are identified in this point cloud.

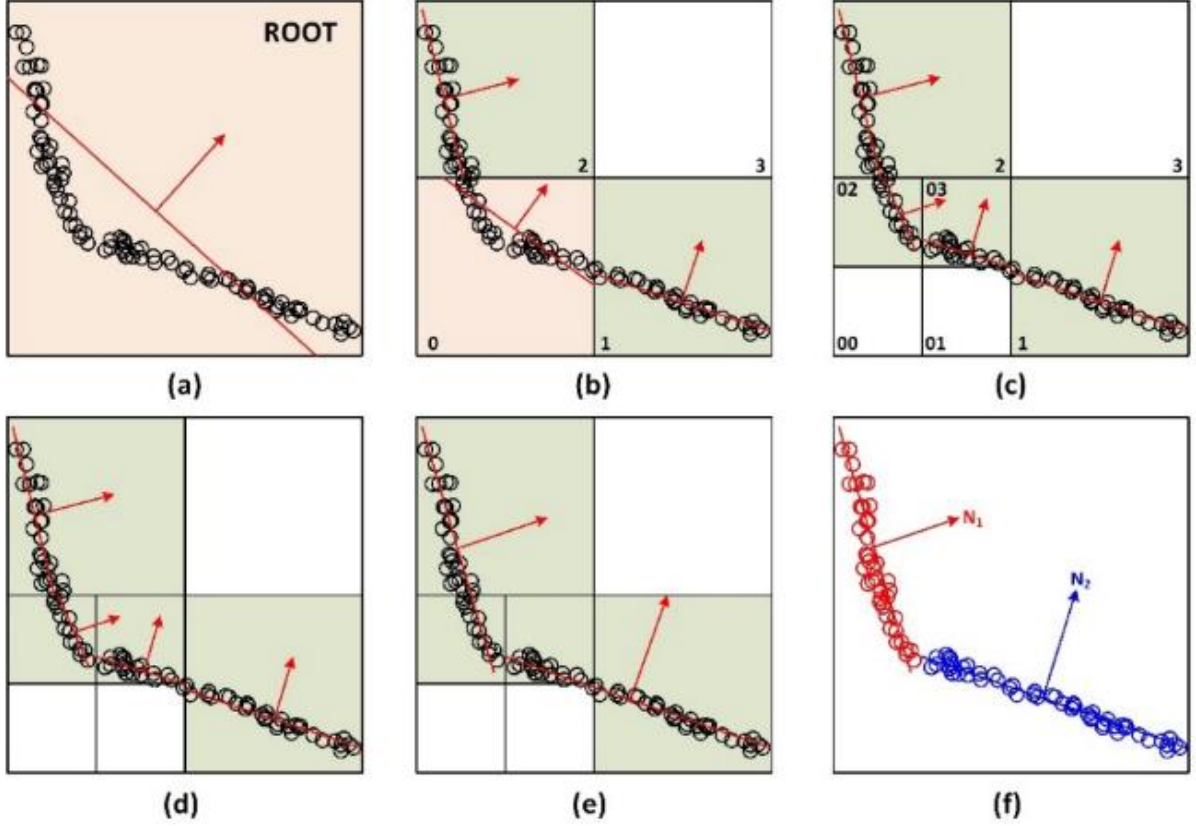


Figure 14 Illustrations for the splitting and merging algorithm

The coplanar criterion is determined using the PCA. The following equations are constructed for PCA computation for the optimal normal of the given data, i.e., points within a node. The solution is obtained from the three eigenvectors. The eigenvectors represent the three axes of the points, while the eigenvalues denote the square sum of points deviating along the corresponding axis. Therefore, the minimum eigenvalue represents the variation along the normal direction of the best-estimated plane using the points within each node.

$$C = \frac{1}{k} \sum_{i=1}^k (\mathbf{p}_i - \bar{\mathbf{p}}) \cdot (\mathbf{p}_i - \bar{\mathbf{p}})^T, \quad C \cdot \vec{v}_j = \lambda_j \cdot \vec{v}_j, j \in \{0,1,2\}$$

where k is the number of points in the point cloud \mathbf{p}_i , $\bar{\mathbf{p}}$ is the centroid of the cluster, λ_j is the j th eigenvalue of the covariance matrix C and \vec{v}_j is the j th eigenvector. Coplanar points should result in very small variation along the normal direction of the estimated plane. Therefore, the coplanar criterion is defined as $\min(\lambda_j) \leq \Delta$. The selection of the threshold Δ is determined by the systematic range measurement error of the LiDAR sensor. Figure 15 shows an example of the strip-based sidewalk extraction results. The direction of the arrows shown in Figure 15 represents the normal direction of the plane, and the magnitude of the arrows represents the

confidence of the detected plane. It can be observed that the man-made surfaces (e.g., pavement or sidewalk) show much higher confidence than the natural surfaces (e.g., grass) where the terrain may slightly distort the surface within the stripe. After all the stripes are processed, the segmentation results are clustered longitudinally based on the k-nearest neighbor (k-NN) method (Ai and Tsai, 2016b; Tsai et al., 2013).

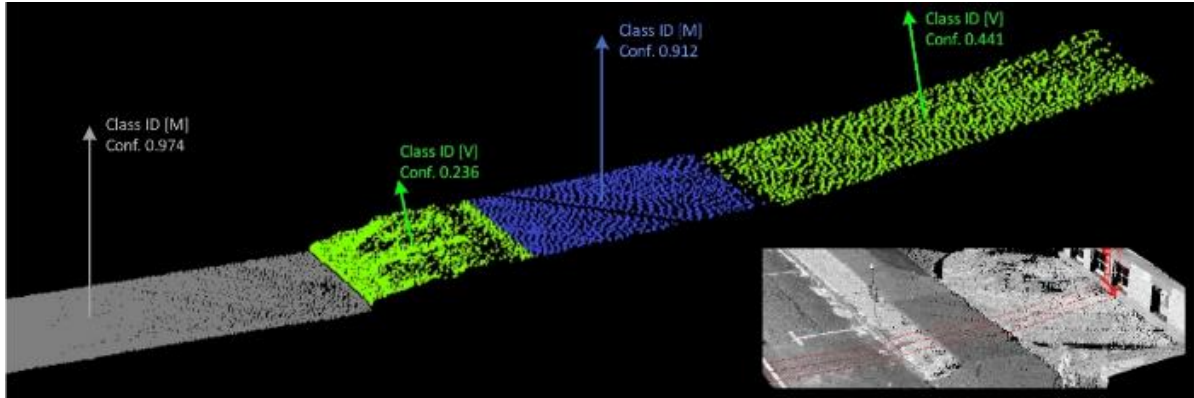


Figure 15 An example of the strip-based sidewalk extraction results

2.5 Curb Ramp Extraction

Although curb ramps have unique features, such as shoulder ramps and center ramp patches with truncated dome bumps, their diverse appearances and designs make it challenging to implement a fully automated curb ramp extraction method. Therefore, this study introduces a semi-automatic approach, including an existing automatic curb ramp extraction algorithm and a manual curb extraction tool.

2.5.1 Automated Curb Ramp Extraction

As suggested in the literature review, the research team directly adopted an existing curb ramp extraction algorithm developed by Hara et al. (2013, 2014) and implemented by Ai and Tsai (2016b) based on the Deformable Part Model (DPM) (P. Felzenszwalb et al. 2008). The DPM algorithm consists of two primary steps: a coarse model (i.e., root filter) and a fine model (i.e., parts filter). Originally, the DPM was proposed for human extraction and pose estimation, where the root filter captures the overall body outlook from the image, and the parts filter captures the individual parts of the human body. In this study, the root filter captures the overall appearance of a curb ramp (as shown in Figure 16 in blue) while the parts filter captures the individual components of a curb ramp (as shown in Figure 16 in orange).

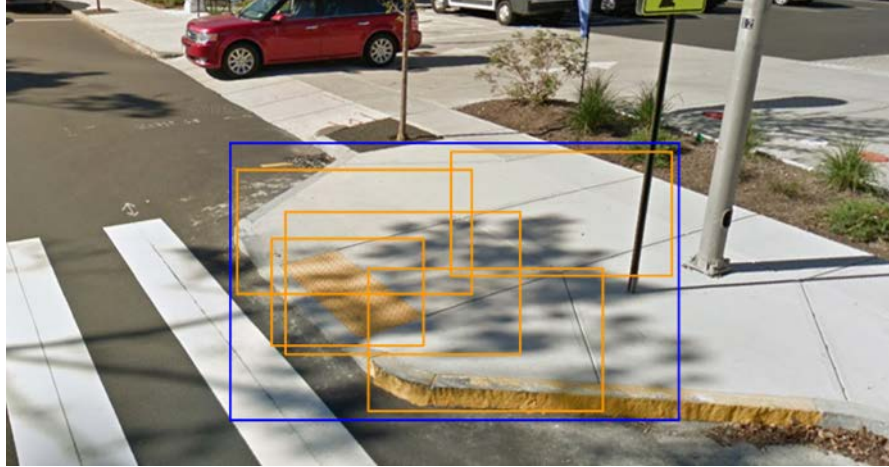


Figure 16 Illustrations of the results from the root filter (blue) and parts filter (orange)

2.5.2 Manual Curb Ramp Extraction

In this study, an efficient manual curb extraction tool using Potree (Schutz, 2016) was developed to review, update, and edit the automated curb ramp extraction results. Potree is a JavaScript-programmed, octree-enabled, web-based library that can efficiently visualize the raw point cloud data and then conveniently annotate the point cloud using tools, such as a bounding box, polyline contour, etc. so that all the curb ramps can be reliably and efficiently detected. Figure 17 shows the interface of the manual curb ramp extraction tool, with a curb ramp manually labeled.

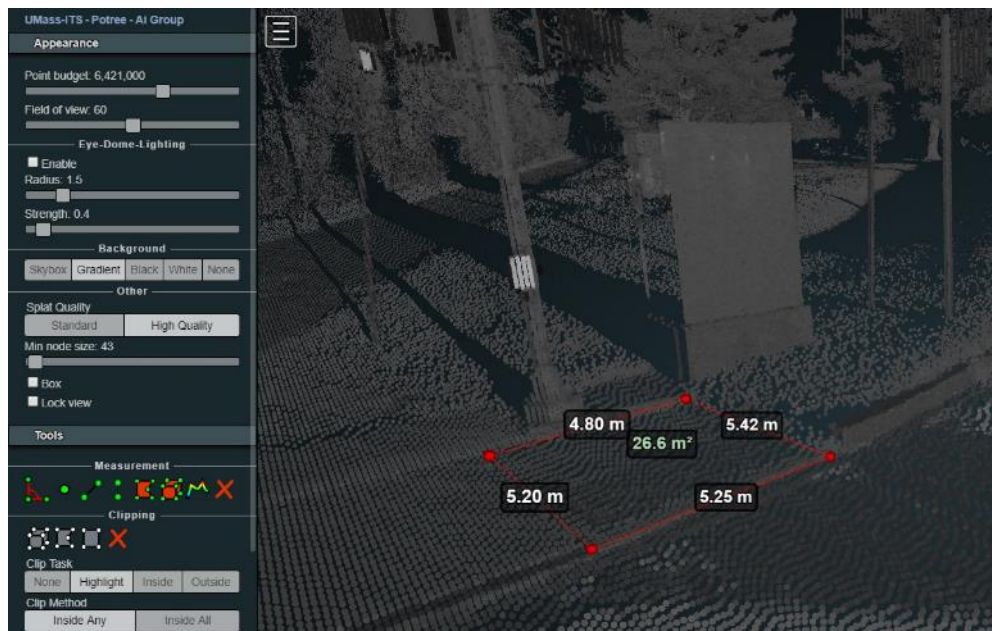


Figure 17 The interface of the manual curb ramp extraction tool

2.6 Key Feature Measurement

The key feature measurements of interest in this study include sidewalk width, cross slope, and grade, and curb ramp slope (running slope). In this subsection, the key features associated with the sidewalk and curb ramp are discussed, respectively.

2.6.1 Sidewalk Features

The key features of interest for the sidewalk, including width, cross slope, and grade, are linear features that require continuous measurements. In this study, an interval of 10 ft. was selected for sampling the width and cross slope measurement to balance the detail and redundancy of the measurements, while an interval of 40 ft. was selected for sampling the grade measurement to avoid measuring a local deformation instead of the actual elevation changes along the longitudinal direction. Figure 18 illustrates how a single measurement was conducted.

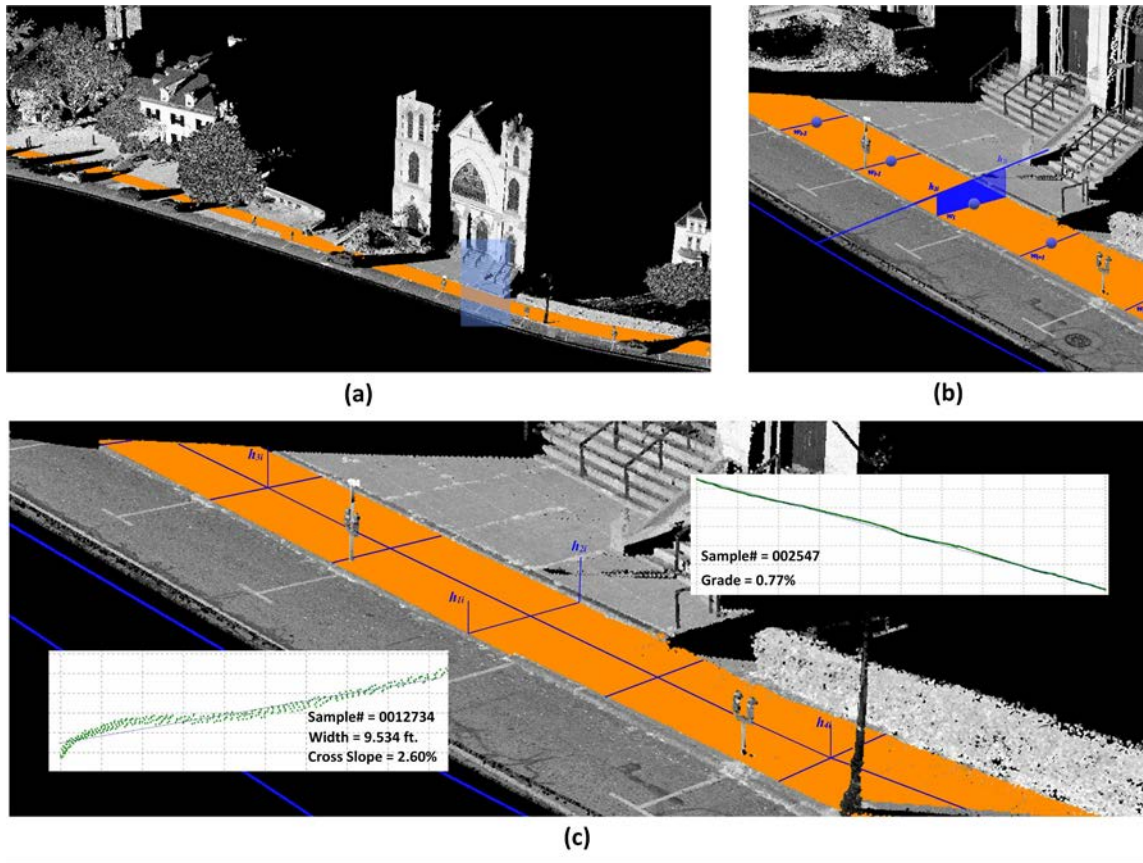


Figure 18 Illustrations of the sidewalk measurements for width, cross slope, and grade

Each blue dot shown in Figure 18 represents an anchoring point with a fixed interval of 10 ft. At each anchor point, the width is measured between the two intersection points h_1 and h_2 .

Both points are the intersecting points between the boundary of the detected sidewalk and the vector that is perpendicular to the data collection trajectory (i.e., the blue line shown in Figure 18). The x-y distance between h1 and h2 are recorded as the width of the sidewalk at the current anchoring point, whereas the linear regression result from all the points between h1 and h2 (with a buffer of a narrow strip of 3 ft.) is recorded as the cross slope at the current anchoring point. Similarly, for every four anchoring points (i.e., every 40 ft.), the grade is recorded based on the linear regression results from all the points between h3 and h4 (with a buffer of a narrow strip of 1 ft.).

2.6.2 Curb Ramp Feature

The key feature of interest for curb ramps, the slope, is defined as the running slope at a curb ramp, as shown in Figure 19. However, the detected curb ramp contains more than just the running slopes, because the landing slope and flare slope may be included in the extraction results, as shown in Figure 19. Therefore, in this study, a similar splitting and merging algorithm, as proposed in Section 2.4, is applied to all the detected curb ramp-associated point clouds for further segmentation into distinctive sloped sections. Figure 19 shows the three examples of the detected curb ramps with different sloped sections.

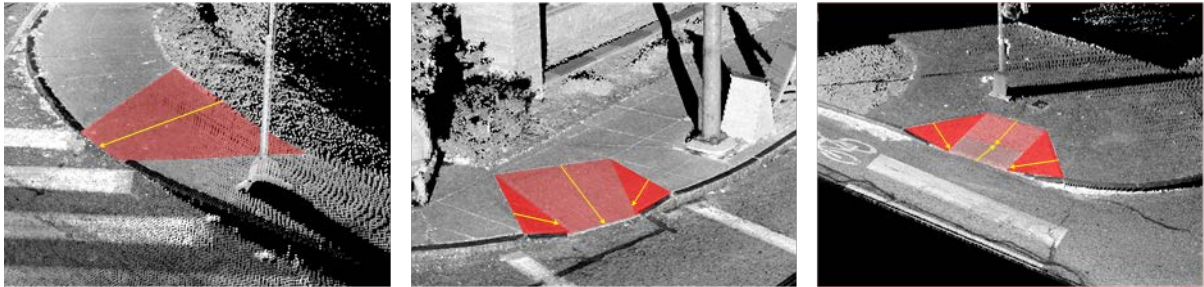


Figure 19 Examples for various running slopes of curb ramps

In Figure 19(a), only one sloped section is identified. Therefore, the running slope is computed based on the only deviation angle from the normal direction of the surface to the vertical direction. In Figure 19(b) and (c), three or more sloped sections are identified. Therefore, the running slope is computed based on the deviation angle from the normal direction of the largest surface in the area to the vertical direction.

3 Results

3.1 Results of Acquired Data

Using the vertical configuration as presented in Section 2.3, the complete State Route 9 corridor was collected in three separate runs to ensure the entirety and the quality of the data, in cases that the data collections were occasionally affected by heavy traffic (i.e., occlusion of the point cloud) or poor weather (i.e., heavy fog and rain). Figure 20 shows an example of the collected point cloud data with a zoom-in view of the pedestrian facilities. The final dataset was prepared by merging different data acquisition sessions for the complete State Route 9, which consists of approximately 8 billion LiDAR points and covers all 271.76 miles of the corridor.

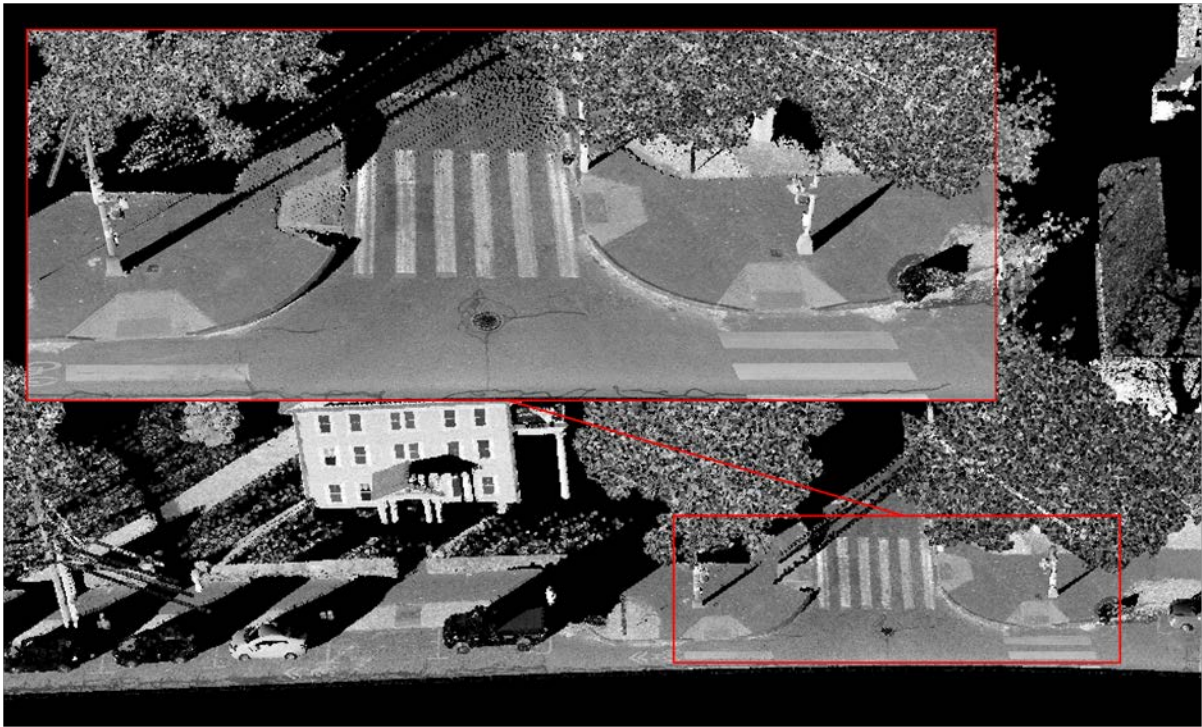


Figure 20 An example of the collected mobile LiDAR point cloud

3.2 Results for Sidewalk Inventory

The objectives of the sidewalk inventory are threefold: 1) verify the sidewalks located in the existing inventory dataset, 2) update sidewalk width, and cross slope at 10 ft. intervals, and 3)

understand the feasibility and productivity of the proposed method. The results for the sidewalk inventory with respect to those three objectives are as follows.

3.2.1 Updated Sidewalk Locations

Complete sidewalk inventory results were obtained using the proposed method from the State Route 9 corridor for both bounds, covering more than 85 miles of sidewalks. Figure 21 shows several examples of the inventoried sidewalk in urban, suburban, and rural areas, where the red polyline layer highlights the detected sidewalk (including the boundaries) using the proposed method in this study, while the yellow and green polyline layers highlight the inventoried sidewalk in the existing dataset from MassDOT. Several key findings were revealed:

1. **Completeness of the dataset:** The existing sidewalk inventory records approx. 76.8 miles of sidewalk from both bounds of the State Route 9, while the results obtained from the proposed method covers approx. 85.1 miles of sidewalk from both bounds. A detailed investigation revealed that many sections of the sidewalk were not inventoried. The newly inventoried sections are attributed to two primary reasons: 1) there are multiple newly built sidewalks that were not updated in the existing database, and 2) there are multiple sections of sidewalks on one bound that were not inventoried. While the overall existing sidewalk inventory shows a relatively high level of completeness, the inventory results obtained from the proposed method shows a significantly higher level of completeness. A complete manual review is still required for a full inventory of the sidewalk, but as the proposed method can accurately extract 94.3% of the sidewalk, the manual intervention becomes negligible
2. **Sidewalk path vs. Sidewalk:** It can be observed that the existing sidewalk inventory collected sidewalk paths instead of the paved sidewalks. A sidewalk path represents the pathway that a pedestrian or a wheelchair user can travel upon, including both the sidewalk and the connectors such as crosswalks and driveways. Therefore, the existing sidewalk inventory contains connected, continuous sections instead of fragmented sections. On the other hand, the proposed method only extracts the sidewalk sections without identifying the connectors due to the nature of the LiDAR segmentation and sidewalk extraction algorithms. Therefore, the new sidewalk inventory contains many small sections that are separated by the connectors. From a planning perspective (taking into consideration connectivity, accessibility, etc.), identifying the sidewalk path may serve a better purpose. However, from a maintenance perspective, identifying the exact locations of the paved sidewalk may serve a better purpose. Therefore, in addition to the updated sidewalk inventory, the research team also developed a separate method for identifying the cross work and driveway, so that these connectors for completing the sidewalk path can be extracted into separate geodatabases. Therefore, by merging or splitting the sidewalk

inventory data layer and the sidewalk path inventory data layer, the newly obtained geodatabase could provide better support for both planning and maintenance needs.

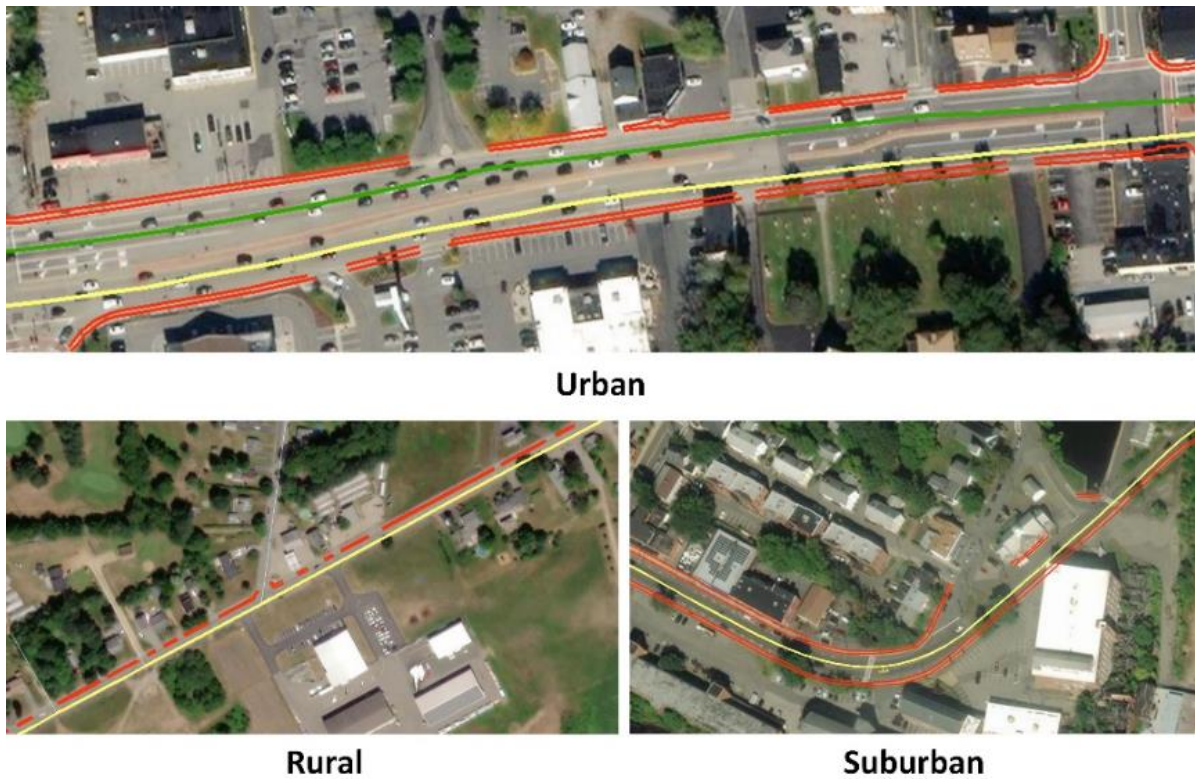


Figure 21 Example of the detected sidewalks in the urban, suburban and rural regions

3. Missing sections: Through a thorough review of the obtained results from the proposed method, there are only a few sections that were missed by the algorithms. These missing sections are attributed to the excessive occlusion due to densely parked vehicles or heavy pedestrian volume. Such an issue can be overcome by multiple data collection sessions and better data collection schedule. In addition, it should be noted that the data collection in this study was conducted using a passenger vehicle with a sensor installation height of 5 ft. A higher installation height could avoid many potential obstructions in the future.

3.2.2 Updated Sidewalk Measures

With the updated sidewalk locations using the proposed method, the corresponding widths, cross slopes, and grades were measured at the intervals of 10 ft. and 40 ft., respectively. Figure 22 shows an example of the measurements along a small section of 1000 ft. It can be observed that in this section, the sidewalk width is consistently around 6.5 ft. with minimum variance, while the cross slopes may vary from 0.4% to 0.6%, and the grade was slightly uphill across

the section varying from 0.2% to 0.5%. Each yellow dot represents a record in the point feature class that consists of a set of measurements.

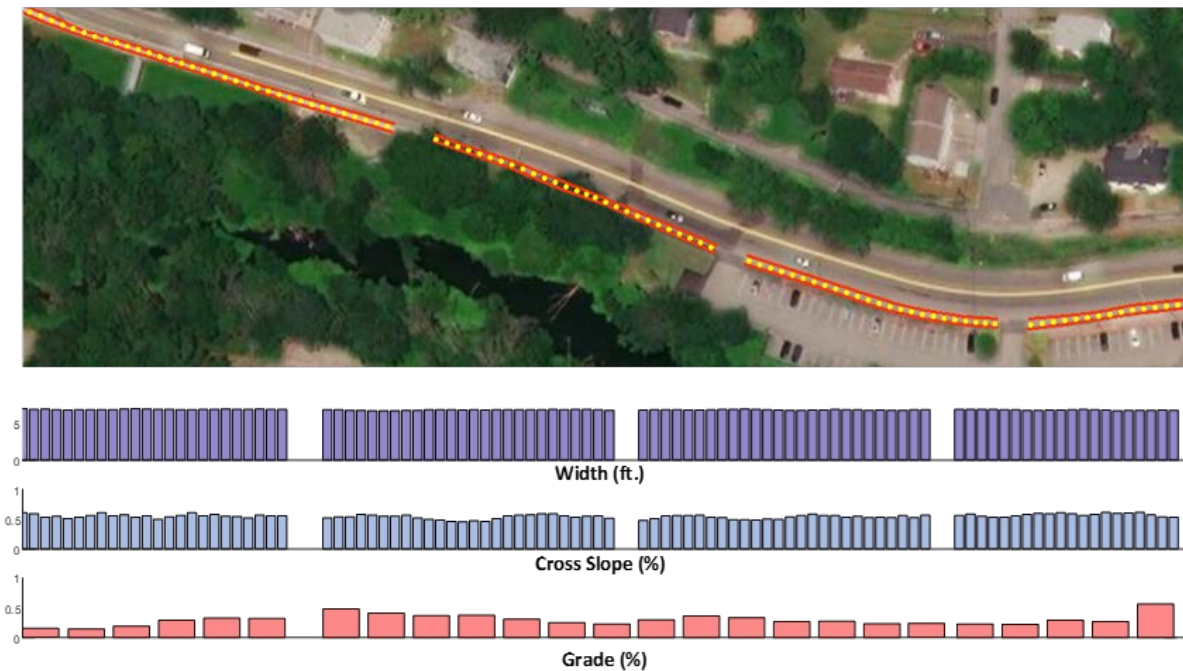


Figure 22 An example of the measurements along a 1000-ft. section

Along the entire State Route 9 corridor, the sidewalk width varies from 3.3 ft. (which requires attention for further improvement) to 14 ft. (which provides abundant width for wheelchair users and pedestrians), while the sidewalk cross slope varies from 2.5% (requiring attention for further safety improvement) to -0.7% (may require drainage improvement). With a dedicated georeferenced layer of sidewalk measurements at 10 ft. and 40 ft. intervals, it becomes very convenient for MassDOT to identify the sections that may require further investigation or improvement. The research team prepared the complete sidewalk inventory results in a file geodatabase that consists of one polyline-feature class (sidewalk location), two point-feature classes (10 ft. measurements for the width and cross slope, and 40 ft. measurements for a grade).

3.2.3 Feasibility and Productivity

The updated sidewalk locations and measurements provide MassDOT a convenient sidewalk inventory dataset for filtering through sections of interest and sections for improvement. While the proposed method shows improved results with location and measurement accuracy, the objective of this subsection is to evaluate whether the proposed method is productively feasible for practical uses if it is implemented on a larger network.

In this study, the entire State Route 9 in Massachusetts, covering all 271.76 miles of the road networks, were processed. Along the State Route 9 corridor, more than 85 miles of sidewalk locations were identified. Using a conventional work-station (with Intel i7-8700 CPU, NVIDIA GeForce GTX 1080 and TensorFlow 1.8), the proposed method created the complete sidewalk inventory along the corridor in less than 30 hours, which can be translated into a processing speed of approximately 6.5 min/mile (or 0.2 million pts/sec). As mentioned above, although a full manual review is still required for a full inventory, the 94.3% accuracy of the proposed method affords a minimal effort during the manual review (i.e., minimal digitization) of less than 2 hours; that can be translated into the review speed of approximately 0.5 min/mile. With parallelization of the program on multiple CPUs and GPUs, it is anticipated that the proposed method has the potential to at least achieve a faster processing speed than the current data acquisition (i.e., 1.5 min/mile at 40mph). For example, if a Quad-GPU configuration is built for processing the point cloud data, it is anticipated that the processing speed would be close to 1.7 min/mile.

Comparing the manual digitization from satellite imagery and field survey, the proposed method provides a feasible solution to accurately and efficiently inventory the network-level sidewalk information. Moreover, the proposed method has the capacity to obtain the width, cross slope, and grade information at a dense interval of 10ft. and 40ft. respectively, which was previously not possible.

3.3 Results for Curb Ramp Inventory

3.3.1 Updated Curb Ramp Locations

The current curb ramp inventory effort made by MassDOT includes a geodatabase that contains 1,283 locations of curb ramps along State Route 9, as shown in Figure 6. In this study, the proposed semi-automated curb ramp extraction algorithm was applied to update the locations of the existing inventory (i.e., to add newly identified curb ramps and to remove redundant or misclassified curb ramps), and to update the running slope information for the validated inventory.

An addition of 17 curb ramps was newly identified by the proposed method, and 3 inventory curb ramps were removed, which formed a complete curb ramp inventory that consists of 1,297 entries. In addition, the proposed method automatically updated 345 locations of the existing inventory with new x-y coordinates that are consistent with the collected LiDAR point cloud data. Figure 23 shows an example of the update, where dark blue dots represent the updated locations, and light blue dots represent the original locations. It can be observed that the location identified by the proposed method is consistent with the ESRI imagery; while the

original location was slightly offset, which may be skewed due to the conversion of the satellite images and the GPS records from the field survey.

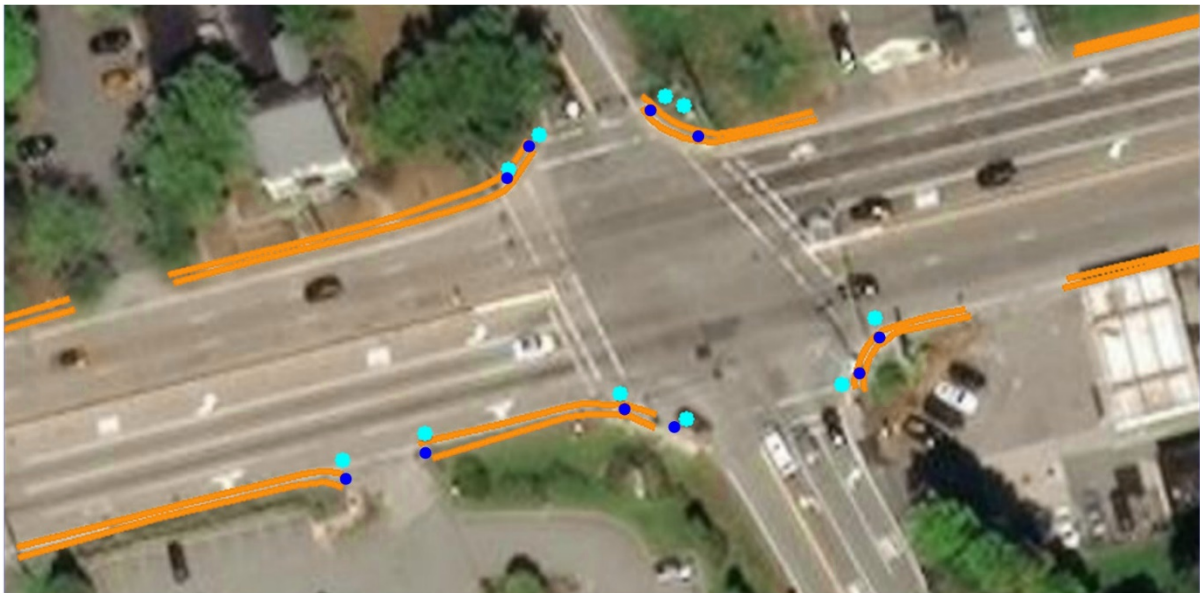


Figure 23 An example of the updated curb ramp locations

For measuring the running slopes of the inventoried curb ramps, the proposed method automatically measured all 1,297 curb ramps and generated the measurements for running slopes, which ranged from 2.7% to 9.3%. Although a further on-field investigation is still needed, the locations where running slopes are greater than 8.3% are recommended for further attention and inspection. While no field survey was carried out as part of this study due to the limitation of the funding and time frame, previous studies by the PI and his research team has validated the LiDAR-based method can achieve a running slope accuracy with an error rate of 0.1% in comparison to the previous study by Ai and Tsai, 2016b. The research team prepared the complete curb ramp inventory results in a file geodatabase that consists of one point-feature class (curb ramp location and measurements).

3.3.2 Feasibility and Productivity

Although the curb ramp inventory and measurement include a semi-automated extraction method that requires manual intervention after the automated algorithm completes its processing, the overall productivity of the process remains encouraging thanks to the convenient tool developed based in Potree. In this study, the entire State Route 9 in Massachusetts, covering 271.76 miles of the road networks, was processed. Along the State Route 9 corridor, 1,297 curb ramps were identified or updated using the same conventional workstation utilized for the sidewalk inventory. Among the 1,297 curb ramps, the fully automated method identified 994, while the manual intervention processed the remaining 303.

It should be noted that although only less than 23.3% of the curb ramps were missing from the automated process, manual intervention is still required to review the entire corridor. Once all the curb ramps were identified, the locations for these ramps and the measurements were automatically populated into the geodatabase. In this study, the proposed method creates the complete curb ramp inventory along the corridor in less than 10 hours; this can be translated into the processing speed of approximately 2.2 min/mile. For each mile of data, the algorithm processed approximately 320 frames of images and the corresponding point cloud in less than 45 seconds, while the remainder of the 87 seconds was spent on the manual intervention using the interactive tool. Comparing with the reported rate of 30 min/curb ramp (Ai and Tsai 2016c) using a field survey method with handheld GPS devices, or 5min/curb ramp (Ai and Tsai 2016c) using a satellite image digitization method, the proposed method provides a more efficient means for network analysis for curb ramp inventory, and more importantly, for accurate curb ramp geometrical measurement.

This page left blank intentionally.

4 Conclusion

This study presents a new pedestrian infrastructure inventory and geometry measurement method by leveraging emerging mobile LiDAR, deep learning, and computer vision technologies. The method consists of two computer-aided algorithms with measurements for sidewalk inventory and curb ramp inventory and was validated on the complete State Route 9 corridor for its network-level feasibility.

The proposed method automatically processed State Route 9 in Massachusetts, covering 271.76 miles of its road networks using a conventional workstation. The results of this study show that the proposed method is a feasible means for a large-scale pedestrian infrastructure inventory, both in terms of accuracy and efficiency. **Two complete geodatabases for sidewalk inventory and measurement and for curb ramp inventory and measurement were generated using the proposed methods.**

The results show that mobile LiDAR is an effective and efficient technology for network-level pedestrian infrastructure inventory:

1. The derived sidewalk inventory geodatabase consists of one polyline-feature class for sidewalk locations, and two point-feature classes for width and cross slope measurements (10 ft. interval), and grade measurements (40 ft. interval). Along the entire State Route 9 corridor, more than 85 miles of sidewalk were identified and updated with the existing inventory.
 - a. The sidewalk width varies from 3.3 ft. that requires attention for further widening improvement to 14 ft. that provides abundant width for wheelchair users and pedestrians, while the sidewalk cross slope varies from 2.5% that requires attention for further safety improvement to -0.7% that may require for drainage improvement;
 - b. The proposed sidewalk extraction and measurement algorithm automatically generated the complete sidewalk inventory along the corridor in less than 30 hours, followed by a manual review that only requires an additional 2 hours.
2. The curb ramp inventory geodatabase consists of one point-feature class for curb ramp locations and measurements. Along State Route 9, a total 1,297 curb ramps were identified and updated with the existing inventory.
 - a. Along the entire State Route 9 corridor, the running slope of curb ramps ranges from 2.7%, which provides a comfortable riding or walking experience, to 9.3% which may require further improvement for landing safety;
 - b. The proposed curb ramp extraction and measurement algorithm automatically generates the complete curb inventory along the corridor in less than 3 hours,

followed by a manual review and update that only requires an additional 7 hours.

3. With the clear demonstration of the feasibility of using mobile LiDAR data for pedestrian infrastructure inventory, the research team recommends implementing the proposed method for a pedestrian infrastructure inventory on a larger network.

The research team developed a complete point cloud processing pipeline (algorithms, tools, and procedures) for pedestrian infrastructure inventory and many other critical transportation assets.

1. In this study, the computer-aided algorithms for both sidewalk inventory and curb ramp inventory were established upon the existing method developed by Ai and Tsai (2016c). The research team further improved the algorithms by addressing the technical challenges in this method, including 1) the existing method relies on strong priors, such as sensor configuration and scene context, to tune the parameters for consistent results; 2) the method can only handle simple scenes where features of interest are significant; 3) the method relies on an iterative or sequential search and a tedious matching strategy for feature extraction. In particular, the PointNet++-based LiDAR segmentation algorithm proposed in this study was not only intended for sidewalk extraction but also to lay a strong foundation for a generalized, LiDAR-based, deep-learning-enabled transportation infrastructure inventory framework. The general framework for the segmentation can be tailored towards facilitating other critical transportation infrastructure and asset extraction with minimum changes.
2. In addition to the two computer-aided algorithms for sidewalk and curb ramp inventories, a manual LiDAR point cloud processing interface was also developed to complement the automated curb ramp extraction algorithm, as well as to provide a convenient tool to visualize, update and edit the sidewalk and curb ramp inventory information. It should be noted that this Potree-based LiDAR point cloud processing interface was not only intended for sidewalk and curb ramp measurement or result review, but also to lay a strong foundation for facilitating a simple, yet powerful interactive LiDAR point cloud processing tool. This would allow it to be easily utilized by MassDOT for visualizing, reviewing, and editing the LiDAR point cloud or point cloud-derived information without the hassle of configuring complex workstation environment.
3. With the establishment of the mobile LiDAR processing pipeline (algorithms, tools, and procedures), the research team recommends gaining more insight into using mobile LiDAR data to conduct inventory and condition evaluations for other critical transportation infrastructure and assets, including pavement marking, signage, guardrail, etc., to increase the positive impact the technology will have in subsequent uses.

5 References

1. Ai, C., and Tsai, Y. J. (2016a). “An automated sign retroreflectivity condition evaluation methodology using mobile LIDAR and computer vision.” *Transportation Research Part C: Emerging Technologies*, 63, 96–113.
2. Ai, C., and Tsai, Y. (James). (2016b). “Automated Sidewalk Assessment Method for Americans with Disabilities Act Compliance Using Three-Dimensional Mobile Lidar.” *Transportation Research Record: Journal of the Transportation Research Board*, 2542(1), 25–32.
3. Ai, C., and Tsai, Y. (James). (2016c). “Automated Sidewalk Assessment Method for Americans with Disabilities Act Compliance Using Three-Dimensional Mobile Lidar.” *Transportation Research Record*, 2542(1), 25–32.
4. Balado, J., Díaz-Vilariño, L., Arias, P., and González-Jorge, H. (2018). “Automatic classification of urban ground elements from mobile laser scanning data.” *Automation in Construction*, 86, 226–239.
5. Boston Public Works Department. (2015). “City of Boston sidewalk inventory data.” *Department of Innovation and Technology*, <<https://data.boston.gov/dataset/sidewalk-inventory>>.
6. Burns & McDonnell Engineering Company. (2009). *Public Sidewalk Inventory Analysis Report, Lee’s Summit, Missouri*. Burns & McDonnell Engineering Company, Lee’s Summit, Missouri.
7. Charles, R. Q., Su, H., Kaichun, M., and Guibas, L. J. (2017). “PointNet: Deep Learning on Point Sets for 3D Classification and Segmentation.” *2017 IEEE Conference on Computer Vision and Pattern Recognition (CVPR)*, IEEE, Honolulu, HI, 77–85.
8. The City of Toronto. (2015). “Sidewalk Inventory, City of Toronto, Canada.” *City of Toronto*, <<https://www.toronto.ca/services-payments/streets-parking-transportation/walking-in-toronto/toronto-sidewalk-inventory/>>.
9. Cole, D. W., and Leon, C. D. (2012). *City of Tucson ADA Sidewalk Inventory Study Report*. The City of Tucson, Department of Transportation, Tucson, Arizona, 35.
10. Dahai Guo, Weeks, A., and Klee, H. (2004). “Segmentations of road area in high-resolution images.” *IGARSS 2004. 2004 IEEE International Geoscience and Remote Sensing Symposium*, 3810–3813 vol.6.
11. Data Transfer Solutions, LLC. (2017). *Sidewalk Inventory & Analysis - Executive Summary - Texarkana MPO*. Data Transfer Solutions, LLC, Texarkana, Texas.
12. Department of Public Works. (2013). *City of Rutland Sidewalk Inventory Report*. Department of Public Works, Rutland, Vermont.
13. Department of Transportation. (2016). *Sidewalk Network Inventory and Assessment for the Champaign Urbana Urbanized Area*. Department of Transportation, Champaign-Urbana, Illinois, 136.

14. Gooch, C. (2017). "Mapping Sidewalks, Los Angeles, California." Los Angeles, California.
15. Guo, Z., Zhang, L., and Zhang, D. (2010). "A Completed Modeling of Local Binary Pattern Operator for Texture Classification." *IEEE Transactions on Image Processing*, 19(6), 1657–1663.
16. Hackel, T., Savinov, N., Ladicky, L., Wegner, J. D., Schindler, K., and Pollefeys, M. (2017). "Semantic3D.net: A new Large-scale Point Cloud Classification Benchmark." *ISPRS Annals of the Photogrammetry, Remote Sensing and Spatial Information Sciences*, 91–98.
17. Hara, K., Le, V., Sun, J., Jacobs, D., and Froehlich, J. E. (2013). "Exploring Early Solutions for Automatically Identifying Inaccessible Sidewalks in the Physical World using Google Street View." *HCIC 2013*, 4.
18. Hara, K., Sun, J., Moore, R., Jacobs, D., and Froehlich, J. (2014). "Tohme: detecting curb ramps in google street view using crowdsourcing, computer vision, and machine learning." *Proceedings of the 27th annual ACM symposium on User interface software and technology - UIST '14*, ACM Press, Honolulu, Hawaii, USA, 189–204.
19. Hometown Colorado Initiative. (2015). "City of Lakewood Sidewalk Inventory." Lakewood, Colorado.
20. Liu, F., Li, S., Zhang, L., Zhou, C., Ye, R., Wang, Y., and Lu, J. (2017). "3DCNN-DQN-RNN: A Deep Reinforcement Learning Framework for Semantic Parsing of Large-Scale 3D Point Clouds." 5678–5687.
21. Loewenherz, F. (2010). "Bellevue's ADA Sidewalk and Curb Ramp Compliance Program." (103) 8.
22. Mannik & Smith Group, Inc. (2018). *Ironton Central Business District Sidewalk Inventory*. Mannik & Smith Group, Inc, Ironton, Ohio.
23. Maturana, D., and Scherer, S. (2015). "VoxNet: A 3D Convolutional Neural Network for real-time object recognition." *2015 IEEE/RSJ International Conference on Intelligent Robots and Systems (IROS)*, 922–928.
24. MID-MO Regional Planning Commission. (2014). *Sidewalk Assessment 2013(Updated 2014 for Ashland and Centralia)*. MID-MO Regional Planning Commission, Boone County, Missouri.
25. New Jersey Department of Transportation. (2007). "County Road Sidewalk Inventory, New Jersey." <<https://www.state.nj.us/transportation/refdata/countysidewalks/>>.
26. Ohio Department of Transportation. (2018). "Sidewalk Inventory, Franklin, Delaware, Fairfield, and Licking Counties in Ohio." *Dataset*, <<https://ckan.smartcolumbusos.com/dataset/sidewalk-inventory1>>.
27. P. Felzenszwalb, D. McAllester, and D. Ramanan. (2008). "A discriminatively trained, multiscale, deformable part model." *2008 IEEE Conference on Computer Vision and Pattern Recognition*, 1–8.

28. Planning Department. (2018). *Delaware County Sidewalk Inventory*. Delaware County Planning Department, Delaware County, Pennsylvania.
29. Public Works Department. (2018). Americans with Disabilities Act (ADA) - Sidewalk Transition Plan, Columbia, Missouri. Public Works Department, Columbia, Missouri.
30. Qi, C. R., Yi, L., Su, H., and Guibas, L. J. (2017). "PointNet++: Deep Hierarchical Feature Learning on Point Sets in a Metric Space." *Advances in Neural Information Processing Systems 30*, I. Guyon, U. V. Luxburg, S. Bengio, H. Wallach, R. Fergus, S. Vishwanathan, and R. Garnett, Eds., Curran Associates, Inc., 5099–5108.
31. Schutz, M. (2016). "Potree: Rendering Large Point Clouds in Web Browsers." Master's Thesis, Institute of Computer Graphics and Algorithms, Vienna University of Technology.
32. Soilán, M., Truong-Hong, L., Riveiro, B., and Laefer, D. (2018). "Automatic extraction of road features in urban environments using dense ALS data." *International Journal of Applied Earth Observation and Geoinformation*, 64, 226–236.
33. Street Division, City of San Diego. (2015). "City of San Diego Sidewalk Inventory." <<https://www.sandiego.gov/blog/city-san-diego-sidewalk-inventory>>.
34. Tsai, Y. (James), Ai, C., Wang, Z., and Pitts, E. (2013). "Mobile Cross-Slope Measurement Method Using Lidar Technology." *Transportation Research Record: Journal of the Transportation Research Board*, 2367(1), 53–59.
35. Vo, A.-V., Truong-Hong, L., Laefer, D. F., and Bertolotto, M. (2015). "Octree-based region growing for point cloud segmentation." *ISPRS Journal of Photogrammetry and Remote Sensing*, 104, 88–100.